FINAL REPORT ON

INVESTIGATION OF MECHANICAL PROPERTIES OF CARBON NITRIDE COATINGS BY NANOINDENTATION TECHNIQUE

At

CSIR-NPL (NATIONAL PHYSICAL LABORATORY)

SUBMITTED IN PARTIAL FULFILLMENT FOR AWARD DEGREE OF

BACHELOR OF ENGINEERING

IN

MECHANICAL

BY

VIKRANT DEV RATHORE

SG 14944

DEPARTMENT OF MECHANICAL ENGINEERING

UIET, PANJAB UNIVERSITY SSG REGIONAL CENTRE,

HOSHIARPUR-146021, Punjab (INDIA)

2018

ONE SEMESTER/SIX MONTHS INDUSTRIAL TRAINING JOINING DETAILS
Session: January to June 2018

A. STUDENT DETAILS:

Name	VIKRANT DEV RATHORE
Roll. No.	SG 14944
Branch	B E MECHANICAL
Mob. No.	9871159695
email id	rathore.vikrant@gmail.com

B. INDUSTRY/COMPANY DETAILS:

Name of Industry/Company (With Complete Postal Address)	CSIR - NATIONAL PHYSICAL LABORATORY Dr. KS KRISHAN MARG, NEW DELHI - 110012
Name of Department:	ADVANCED CARBON PRODUCTS
Name and Details of Project Alloted	INVESTIGATION OF MECHANICAL PROPERTIES OF CARBON NITRIDE COATINGS BY NANO INDENTATION TECHNIQUE
Training Timings	9:00 AM - 5:30 PM

B. INDUSTRY/COMPANY TRAINING INCHARGE DETAILS:

Name of Training Incharge	Dr. SREEKUMAR CHOCKALINGAM
Designation	PRINCIPAL SCIENTIST
Department	ADVANCED CARBON PRODUCTS
Contact No.	OFF - +910114560846O MOB - +91 9910801310
email id	sreekuc@nplindia.org

Signature of Authorized Company Official
with Company Seal

Dr. Sanjay R. Dhakate
Senior Principal Scientist
CSIR - National Physical Laboratory
Dr. K.S. Krishan Marg, New Delhi-12

1

CERTIFICATE

Certified that the training report entitled "INVESTIGATION OF MECHANICAL PROPERTIES OF CARBON NITRIDE COATINGS BY NANOINDENTATION TECHNIQUE " submitted by VIKRANT DEV RATHORE (SG 14944), student of Mechanical, UIET, Panjab University Swami Sarvanand Giri Regional Centre, Hoshiarpur, in the partial fulfillment of the requirement for the award of Bachelor of Engineering (Mechanical) Degree of Panjab University, Chandigarh is a record of student's own study carried under my supervision & guidance.

This report has not been submitted to any other university or institution for the award of any degree.

Dr. Sreekumar Chockalingam

Principal Scientist & Associate Professor (AcSIR)

DECLARATION

The work embodied in the training report entitled, INVESTIGATION OF MECHANICAL PROPERTIES OF CARBON NITRIDE COATINGS BY NANOINDENTATION TECHNIQUE submitted to the department of Mechanical Engineering at UIET, Panjab University Swami Sarvanand Giri Regional Centre, Hoshiarpur for the award of degree of Bachelor of Engineering, has been done by me. The training report is entirely based on my own work and not submitted elsewhere for the award of any other degree. All ideas and references have been duly acknowledged.

Vikrant Dev Rathore

B.E Mechanical, 8th semester

SG 14944

Countersigned by:

Dr. Sreekumar Chockalingam

Principal Scientist & Associate Professor (AcSIR)

ABSTRACT

This training report gives a brief introduction to Nanoindentation and its wide range of applications along with uncertainty analysis of mechanical properties that might be present during the Nanoindentation process. The uncertainty analysis also shows that Nanoindentation is an effective technique in determining the mechanical properties of carbon nitride coated samples. Not only does the carbon nitride coating improve mechanical properties like hardness and reduced modulus but also adds aesthetic features as well to the carbon steel sample

Vikrant Dev Rathore

B.E Mechanical 8th semester (2017-2018)

 SG 14944

ACKNOWLEDGEMENTS

Vikrant Dev Rathore

B.E Mechanical 8th semester (2017-2018)

 SG 14944

CONTENTS

LIST OF FIGURES & TABLES

ABOUT CSIR-NPL

The National Physical Laboratory of India, situated in New Delhi, is the measurement standards laboratory of India. It maintains standards of SI units in India and calibrates the national standards of weights and measures.

The National Physical Laboratory, India was set up in 1900) is one of the earliest national laboratories set up under the Council of Scientific & Industrial Research. Jawaharlal Nehrulaid the foundation stone of NPL on 4 January 1947. Dr. K. S. Krishnan was the first Director of the laboratory. The main building of the laboratory was formally opened by Former Deputy Prime Minister Sardar Vallabhbhai Patel on 21 January 1950. Former Prime Minister Indira Gandhi, inaugurated the Silver Jubilee Celebration of the Laboratory on 23 December 1975.

NPL Charter:-

▶ The main aim of the laboratory is to strengthen and advance physics-based research and development for the overall development of science and technology in the country. In particular its objectives are:

▶ To establish, maintain and improve continuously by research, for the benefit of the nation, National Standards of Measurements and to realize the Units based on International System (Under the subordinate Legislations of Weights and Measures Act 1956, reissued in 1988 under the 1976 Act). To identify and conduct after due consideration, research in areas of physics which are most appropriate to the needsof the nation and for advancement of field

▶ To assist industries, national and other agencies in their developmental tasks by precision measurements, calibration, development of devices, processes, and other allied problems related to physics.

▶ To keep itself informed of and study critically the status of physics.

FIGURE N.1: NPL AND CSIR LOGO

Major NPL contributions:

The Indelible Mark/Ink

During general election, nearly 40 million people wear a CSIR mark on their fingers. The Indelible ink used to mark the fingernail of a Voter during general elections is a time-tested gift of CSIR to the spirit of democracy. Developed in 1952, it was first produced in-campus. Subsequently industry has been manufacturing the Ink. It is also exported to Sri Lanka, Indonesia, Turkey and other democracies.

Pristine Air-Quality Monitoring Station at Palampur

National Physical Laboratory (NPL) has established an atmospheric monitoring station in the campus of Institute of Himalayan Bioresource Technology (IHBT) at Palampur (H.P.) at an altitude of 1391 m for generating the base data for atmospheric trace species & properties to serve as reference for comparison of polluted atmosphere in India. At this station, NPL has installed state of art air monitoring system, greenhouse gas measurement system and Raman Lidar. A number of parameters like CO, NO, NO2, NH3, SO2, O3, PM, HC & BC besides CO2 & CH4 are being currently monitored at this station which is also equipped with weather station (AWS) for measurement of weather parameters.

Gold Standard (BND-4201)

The BND-4201 is first Indian reference material for gold of '9999' fineness (gold that is 99.99% pure with impurities of only 100 parts-per-million).

FIGURE N.2: NPL MAIN BUILDING

ADVANCED CARBON PRODUCTS: A leading centre in India dedicated to research in both pure and applied science of Carbon with principal motives i) to develop the process technology of newer carbon products which hold strategic importance and are not available to the country at any cost, ii) to develop products which can be made cost-effective by innovative process suitable to available infrastructure, expertise and resources in India, iii) to promote overall growth of carbon science and technology in the country through sustained R&D, research publications, patents, technology transfer, consultancy to industry, national labs etc.
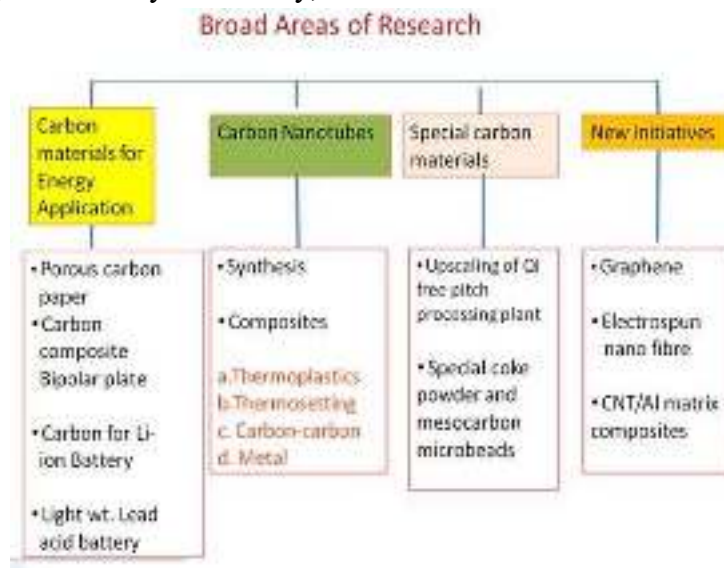
FIGURE N.3 : AREAS OF RESEARCH

CHAPTER 1

INTRODUCTION

Nanoindentation is a type of indentation method done at the Nano scale to measure mechanical properties of small volume. This technique was developed in the mid-1970s.

Applications of nanoindentation

Thin films

MEMS/NEMS testing

Living cells and joints(biological use)

Solid body which applies the load is called indenter.
Solid body which undergoes deformation under the indenter is called the sample.

IMPORTANT MECHANICAL PROPERTIES:

Elasticity: It is the property by virtue of which a material deformed under a load is able to return to its original dimension after the removal of the load.
If body completely regains its shape, it is called perfectly elastic
Elastic Limit marks the partial breakdown of elasticity beyond which removal of load results in a degree of permanent deformation.

Example: Steel, Aluminum, Copper etc. maybe considered perfectly elastic within limits.

Plasticity: The characteristics of the material by which it undergoes inelastic strain beyond those at the elastic limit is known as plasticity.
When large deformation occurs in ductile material loaded in plastic region, the material is said to undergo plastic flow.
Used in pressing and forging

Ductility: The property which allows a material to be drawn out longitudinally to a reduced section, under action of tensile force.
High degree of plasticity and strength, low degree of elasticity.
Used in wire drawing.

Brittleness: It is the lack of ductility. It cannot be drawn out by tension to smaller section
Failure takes place under load without significant deformation.
Ordinary Glass is nearly brittle.

Example: Cast Iron, concrete, ceramic material are brittle in nature.

Malleability: It is the property of a material which permits the material to be extended in all directions without rupture.
A malleable material possesses a high degree of plasticity but not necessarily great strength.

Toughness: Property of material which enables it to absorb energy without fracture.
   1. Desirable in material which is subjected to cyclic/shock loading.
   2. Represented by area under stress strain curve for material up to fracture.
   3. Bend test used for common comparative test for toughness.

Hardness: It is the ability of a material to resist indentation or surface abrasion.
   1. Brinell hardness test is used to check hardness.

Strength: This property enables material to resist fracture under load.
   1. Important for design point of view.
   2. Load required to cause fracture divided by area of specimen is termed as ultimate strength.

Stress: Resistance offered by body to deformation.
   1. Engineering stress=load/original area

Strain: Deformation per unit length in direction of deformation is known as strain.

STRESS STRAIN CURVE:

OA : Proportional limit
A   : Elastic limit
B   : Yield stress point/upper
        yield stress point
C : Lower yield stress point
D : Ultimate stress point
E : Breaking or rupture point
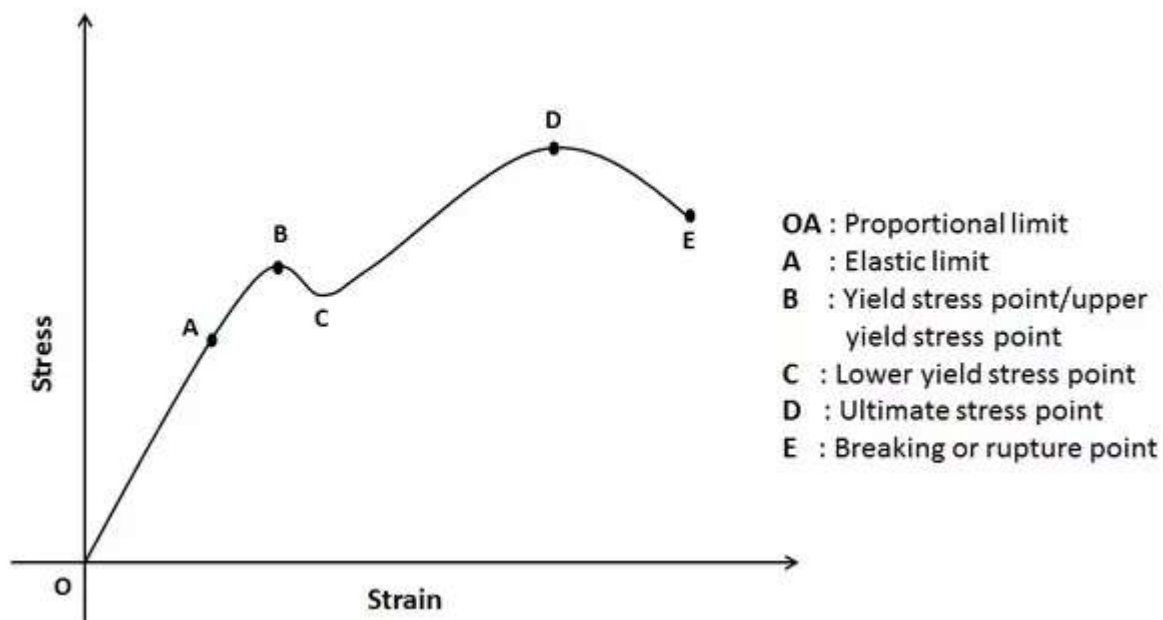
FIGURE 1.1: STRESS STRAIN CURVE

Proportional limit: It is the stress at which the stress strain curve ceases to be straight . Hooke's law for perfectly linear elastic is valid upto proportional limit.

σ= εE

where E is modulus of elasticity.

ε is strain

Elastic limit: Point in the stress strain curve upto which material remains elastic.
Till this point there is no permanent deformation after removal of load.

Yield point: The point beyond elastic limit at which the material undergoes an appreciable increase without further increase in load.

STRESSES:

The term stress has huge importance in this field of research. There are three types of stress. The first is the tensile stress. This type of stress tries to pull the surface apart into at least two parts in two opposite directions. Thus it always acts normal to a given plane. The second is the compressive stress. This type of stress tries to compress the surface from one given or from two given opposite directions. The compressive stress and/or stresses also act(s) normal to a given plane. Such stresses are usually expressed as σ_{xx}, σ_{yy}, and σ_{zz}'.

Therefore, altogether nine components of stresses can act on a solid and may be expressed by a corresponding matrix notation as follows:

$$\begin{bmatrix} \sigma_{xx} & \tau_{xy} & \tau_{xz} \\ \tau_{yx} & \sigma_{yy} & \tau_{yz} \\ \tau_{zx} & \tau_{zy} & \sigma_{zz} \end{bmatrix}$$

The maximum tensile stress due to static contact (σ^s_m) under a normal load (P) in the Hertzian contact situations is calculated:

$$\sigma^s_m = \frac{(1-2v_s)p_0}{2}$$

The corresponding contact radius (as) is given by:

$$a_s = \left(\frac{4}{3}kPrE_s\right)^{\frac{1}{3}}$$

16

r is the radius of the indenter. It typically varies from 150 nm for a sharp Berkovich indenter to about 200 μm for a blunt spherical indenter. Here, E_s is the Young's modulus of the sample, and k is a factor given by:

$$k = \frac{9}{16}\left[(1-v_s^2)+(1-v_i^2)\frac{E_s}{E_i}\right]$$

v_i and E_i are the Poisson's ratio and the Young's modulus of the indenter, respectively, and v_s and E_s are the Poisson's ratio and Young's modulus of the sample. Further, the maximum tensile stresses due to dynamic contact (σ^d_m) between a brittle solid (e.g., a glass surface) and the sliding indenter can be obtained from the following equation :-

$$\sigma^d_m = (1+15.5\mu)\sigma^s_m$$

The values of normalized shear stress (τ') can be estimated at various points in the (r,z) plane in a cylindrical coordinate system using the following equations:-

$$\tau' = \frac{\sigma_1' - \sigma_2'}{2}$$

Here the normalized principal stresses σ'₁ and σ'₃ are given by:-

$$\sigma_1' = \frac{\sigma_r' + \sigma_z'}{2} + \sqrt{\left(\frac{\sigma_r' + \sigma_z'}{2}\right)^2 + \sigma_{rz}'^2}$$

$$\sigma_3' = \frac{\sigma_r' + \sigma_z'}{2} + \sqrt{\left(\frac{\sigma_r' + \sigma_z'}{2}\right)^2 + \sigma_{rz}'^2}$$

CHAPTER 2

MECHANICS OF ELASTIC AND ELASTOPLASTIC CONTACTS

THE DIFFERENT MODELS:

1. Elastic Indentation Model: The Elastic Indentation Model was developed by Hertz in 1882.

In this type of model, the indenter is assumed to be a rigid cone. Any reformation of indenter is insignificant in comparison to that of sample and sample is assumed to be linearly elastic.
Pressure distribution can P(r) can be expressed by:-

$$p(r) = \frac{E \cot \theta}{2(1-v^2)} \cosh^{-1}\left(\frac{a}{r}\right)$$

Where r= radial distance measured from the center of the contact circle of diameter 'a'

E= Young's Modulus

v= Poisson's Ratio of cone

Θ= Semi elliptical angle of cone

using the boundary condition a = r, the mean contact pressure can be written as:-

$$p_m = H = \frac{E \cot \theta}{2(1-v^2)}$$

This quantity, p_m, then can be likened to be the measure of hardness (H) of a linearly elastic solid due to indentation by a perfectly rigid indenter. However, the indenter shape can be of many types, e.g., wedge, spherical, and cylindrical with a flat contact end. In particular, for a spherical indenter of radius R, H can be expressed as a function of the load (P) by equation:-

$$H = \frac{P^{\frac{1}{3}}}{\pi}\left(\frac{4E}{3R(1-v^2)}\right)^{\frac{2}{3}}$$

We have to assume that the friction and the elastic deformation of the indenter are negligible. Now, the impact of the indentation disappears completely after unloading for a perfectly elastic material.

The depth of penetration can be measured from the instrumented hardness testing equipment so that the area can be found from the depth measurement.
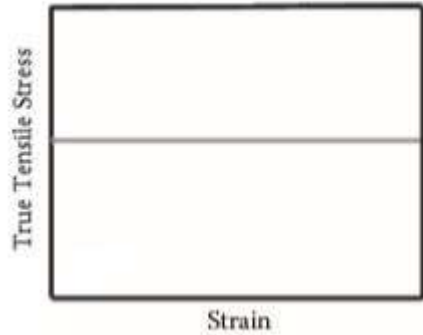
(a)
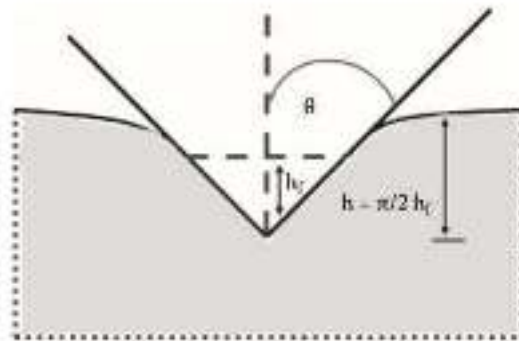
(b)

FIGURE 2.1: (A) STRESS STRAIN CURVE FOR ELASTIC INDENTATION MODEL (B) SCHEMATIC REPRESENTATION OF THE INDENTATION IN AN ELASTIC SOLID

2. The Rigid Perfectly Plastic Model: Prandtl advocated this model, which is based on the slip line field theory.

The indenter was assumed to be perfectly rigid. But, in contrast to the elastic model, here the sample is considered to be rigid and perfectly plastic. It means that no plastic deformation will occur until a limiting or cutoff stress Y is attained. The uniform pressure p across the punch is given by:-

$$p = cY = 2k\left(1 + \frac{\pi}{2}\right)$$

This uniform pressure p can be likened to the hardness, H. Therefore, one can safely assume that, in general, $p = H = cY$, where c is the appropriate constraint factor, depending on the geometry of the indenter and the interfacial friction. For instance, when the stress condition fulfills the Tresca criterion, c will assume the value 2.6. Similarly, when the stress condition fulfills the von Mises criterion, c may be as high as 3.

The most interesting aspect of this model is that even for a sharp contact situation, it can predict hardness values for materials having a high magnitude of the ratio E/Y. However, when the contact situation to be tackled is that of a blunt indenter, the model is not successful in predicting the hardness values of those materials having a relatively lower magnitude of E/Y. In such cases, where there is no friction at the interface between the sample and the rigid wedge-shaped indenter of semi-apical angle θ, the pressure across the face of the indenter is given by:

$$p = 2k(1 + \theta)$$

The material's hardness, H, can be equivalently expressed as:-

$$H = 2k(1 + \theta)$$
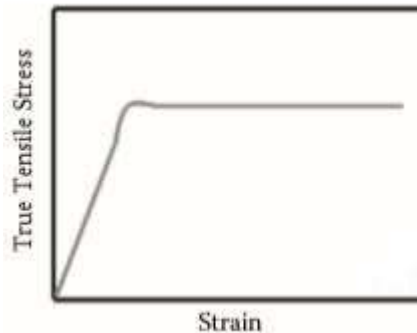
FIGURE 2.2: THE RIGID PERFECTLY PLASTIC MODEL

3. The Spherical-Cavity Expansion Model: The indentation process has been imagined to be like that of a physical expansion of an existing cavity in a given solid under the applied load.

Johnson's analysis has been most successful one for spherical cavity model. The situation closely resembles the indentation of elastic –plastic solids. The results of this model could easily fit materials having high as well as low E/Y values.

To take care of indentation volume, the shape of the indenter comes into picture that represents ratio of hardness(H) to the yield stress(Y).

For conical and pyramidal indenters:-

$$\frac{H}{Y} = \frac{2}{3}\left[1 + \ln\left(\frac{E \cot \theta}{3Y}\right)\right]$$

$$\frac{H}{Y} = \frac{2}{3}\left[1 + \ln\left(\frac{E(a/R)}{3Y}\right)\right]$$

This treatment assumes that the material has a constant yield stress and there is no work hardening produced by the indentation process itself. When the elastic plastic boundary is at a distance C from the center of the contact, the cavity pressure is given by:

$$P = Y\left(\frac{2}{3} + 2\ln\frac{c}{a}\right)$$

When c=a , the contact pressure is given by:

$$P_C = \frac{2}{3}Y$$

Thus, this value of P defines a critical applied pressure Pc required for plastic deformation to occur at all. If the applied pressure P is less than Pc, no plastic deformation occurs. However, it automatically follows that if the indentation pressure is less than Y, no plastic indentation usually takes place.
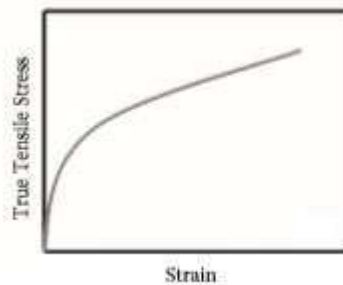
(a)
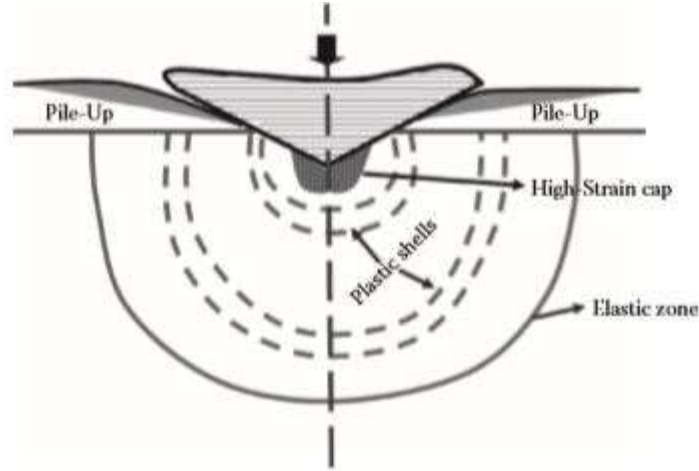
(b)

FIGURE 2.3: (a) THE SPHERICAL-CAVITY EXPANSION MODEL.
(b) SCHEMATIC REPRESENTATION OF THE INDENTATION PROCESS
ACCORDING TO THE SPHERICAL-CAVITY EXPANSION MODEL.

4. The Elastic and Perfectly Plastic Model: The analytical relationship for calculating hardness from the uniaxial material properties and indenter geometry for a wide variety of elastic and plastic materials has been developed using an elastic, perfectly plastic model. From this model, the hardness of a material due to the conical indentation is given by:
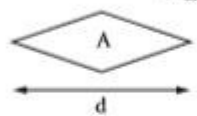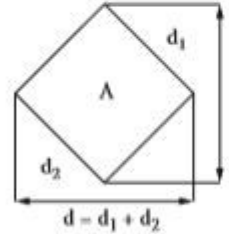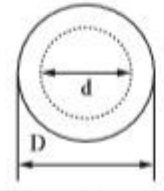
$$H = \frac{E \tan\theta}{2(1-v^2)} \tanh\left(\frac{2(1-v^2)YC_\theta}{E \tan\theta}\right)$$

where $C_\theta = \frac{2}{\sqrt{3}}(2.845 - 0.002\theta)$ and the semi-apical angle of the indenter is in the range of $0° < \theta \le 37.5°$.

CHAPTER 3

INDENTERS, HARDNESS AND ELASTIC MODULUS

TYPES OF INDENTERS:

Comparison of Hardness Evaluation for Four Different Indentation Tests

Method of Testing	Impression Shape	Contact Area	Hardness Value
Berkovich		$A = a^2\sqrt{(3/2)}$	$H_B = F/A$ $= F/a^2\sqrt{(3/2)}$
Knoop		$A = d^2/14.4$	$H_K = F/A$ $= F \times 14.4/d^2$
Vickers		$A = d^2/(2 \times \sin 68°)$ (theoretically, $d_1 = d_2 = d$)	$H_V = F/A$ $= 1.8544 \times F/d^2$
Brinell		$A = [\pi D^2$ $[1 - (1 - (d/D)^2)]^{1/2}]/2$	$H_C = F/A$ $= 2F/[\pi D^2$ $[1 - (1 - (d/D)^2)]^{1/2}]$

Note: F = applied force; A = projected contact area.

FIGURE 3.1: COMARISION OF INDENTERS

Mohs introduced a 10 point scale with 10 being hardest (diamond) amd 1 being the most soft material(talc)

Around 1900, measuring machines for indentation hardness under both static and dynamic conditions become commercially available.

HARDNESS:

Hardness can be defined as the ratio of :-

$$H = \frac{\text{Force, } P}{\text{Contact area, } A}$$

Source	Evolution of Hardness Concepts
Aristotle [1]	Ability of a surface to remain "static" against external stress
Huygens [2]	Easy cleavage plane of calcite excited only for forward movement of knife
Haüy [3]	Mineral classification in accordance with ability to scratch other minerals
Mohs [4, 5]	Introduction of the 10-stage Mohs hardness scale
Seebeck [6]	The first scratch hardness tester with predefined load application
Martens [7]	New scratch hardness tester to measure the scratch width and the normal load
Calvert and Johnson [8]	Depth-controlled conical indentation
Hertz [9]	First quantitative definition of hardness

FIGURE 3.2: DEVELOPMENT OF THE CONCEPT OF HARDNESS

ELASTIC MODULUS:

Elastic modulus in a given direction is always the ratio of stress to strain

$$E_1 = \frac{\sigma}{\left(\frac{l}{l}\right)} \qquad \kappa = \frac{\pm\sigma}{\left(\frac{V}{V}\right)} \qquad \eta = \frac{\chi}{\left(\frac{\theta}{\theta}\right)} \qquad v = \frac{\left(\frac{D}{D}\right)}{\left(\frac{l}{l}\right)}$$

FIGURE 3.3: DEFINITIONS OF ELASTIC MODULI

Here, E_1 is the Young's modulus, σ is the applied tensile stress, $\Delta l/l$ is the increase in length per unit length, κ is the bulk modulus, $\pm\sigma$ is tensile or compressive stress, $\Delta V/V$ is the change in volume per unit volume, η is the shear modulus, χ is the tangential stress, $\Delta\theta/\theta$ is angle of shear or shear strain, v is the Poisson's ratio, and $\Delta D/D$ is the decrease in diameter per unit diameter.

CHAPTER 4

NANOINDENATION MODES

1. Depth Control Mode: frequently used for multilayer thin films. The reason is that it has the ability to measure stiffness at a precision level, a depth of few nanometers

Example : We consider a multilayered thin film architecture(MCTFA) having four layers made of different stiffness values , the continuous stiffness measurement procedure can tell us about the hardness and modulus at each depth with a spacious resolution.

Thus we can get hardness and modulus as a function of depth. CSM technique can be utilized to invest the hardness and modulus of each layer of a magnetic storage device.
Further, a pop in at a certain depth in P-h plot during CSM /progressive load measurement can tell us about the localized fracture strength of thin brittle amorphous carbon film on silicon.
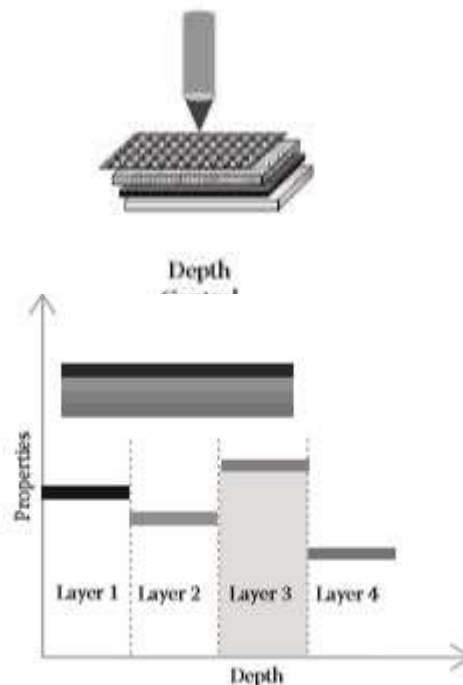
FIGURE 4.1: Depth Control Mode

2. Location Control Mode: In Location control mode, we can measure the local mechanical properties at specific sites as per choice. To measure the nanomechanical properties of a grain boundary; a coating substrate interface far away from or very near to a pole in porous structure; the interference of a weld zone, the interface of matrix and fiber etc.
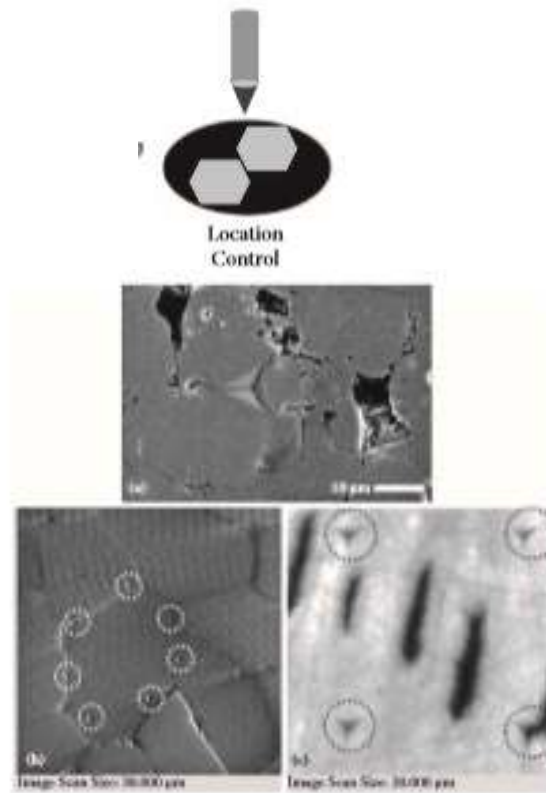
FIGURE 4.2: Location-specific nanoindentation: (a) on plasma-sprayed HAp coating showing footprint of indentation avoiding defects, (b) on a grain boundary and very near to a grain boundary region of dense alumina ceramics, and (c) very near, near, and far away from dentin tubules.

3. Phase Control Mode: In Phase control mode, the nanoindentation technique can be used to evaluate the mechanical properties on individual phases in a multiphase material.

It is necessary to identify the phases by using an optical or scanning probe microscope facility equipped with a nanoindenter.
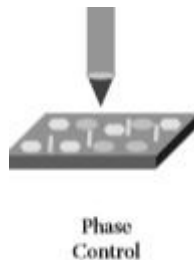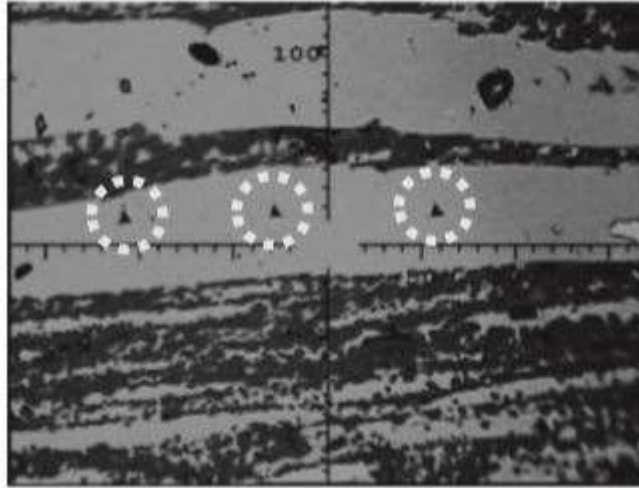
FIGURE 4.3: PHASE-SPECIFIC NANOINDENTATION ON A BIPHASIC CERAMIC MATERIAL.

4. In- situ Nanoindentation: In this technique , a very specially designed nanoindentation tip along with sensing devices for ultra-low load and depth are used under very high vacuum condition inside the chamber of a scanning(SEM) or transmission electron microscope (TEM) so that it becomes possible to observe, investigate and measure the deformation at the nanoscale in situ real time.

CHAPTER 5

NANOINDENTATION ANALYSIS MODEL

1. Oliver- Pharr Model: One of the most widely accepted models for nanoindentation behavior of brittle solids. This model treats the unloading curve as the consequence of a fully elastic contact event.

Assumptions are:

1. . Deformation upon unloading is purely elastic.

2. The compliance of the sample and of the indenter tip can be combined as springs in series, e.g.,

$$\frac{1}{E_r} = \left(\frac{1-v_s^2}{E_s}\right) + \left(\frac{1-v_i^2}{E_i}\right)$$

where, Er is the reduced modulus, E is the Young's modulus, v is the Poisson's ratio, and subscripts i and s refer to the indenter and sample, respectively.

For Ideal Berkovich Indenter $A_c = 24.5 h_c^2$

Analytical Model – Oliver and Pharr

$$P = \alpha(h - h_f)^m$$

$$h_c = h_t - \varepsilon\frac{P}{S}$$

$$A_c = f(h_c)$$
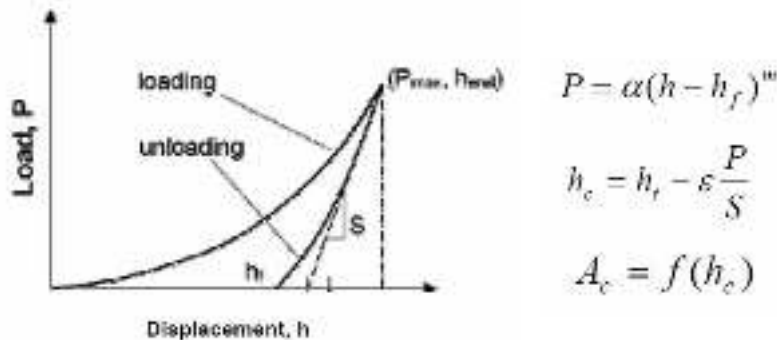
FIGURE 5.1 : OLIVER PHARR MODEL

2. Doerner- Nix Model: They presented the first complete nanoindentation data analysis. They argued that the indenter can be treated as a flat punch as long as the change in contact area is small during unloading.

Assumptions:

 As long as loading process happens all of the material in contact with the indenter is plastically deformed.
Outside the contact impression of the indents, elastic deformation occurs at the surface.

Using these two assumptions, the model develops the connection between p-h data and contact area.

Analytical Model – Doerner-Nix Model

$$A_c = f(h_c) \qquad\qquad H = \frac{P_{max}}{A_c}$$
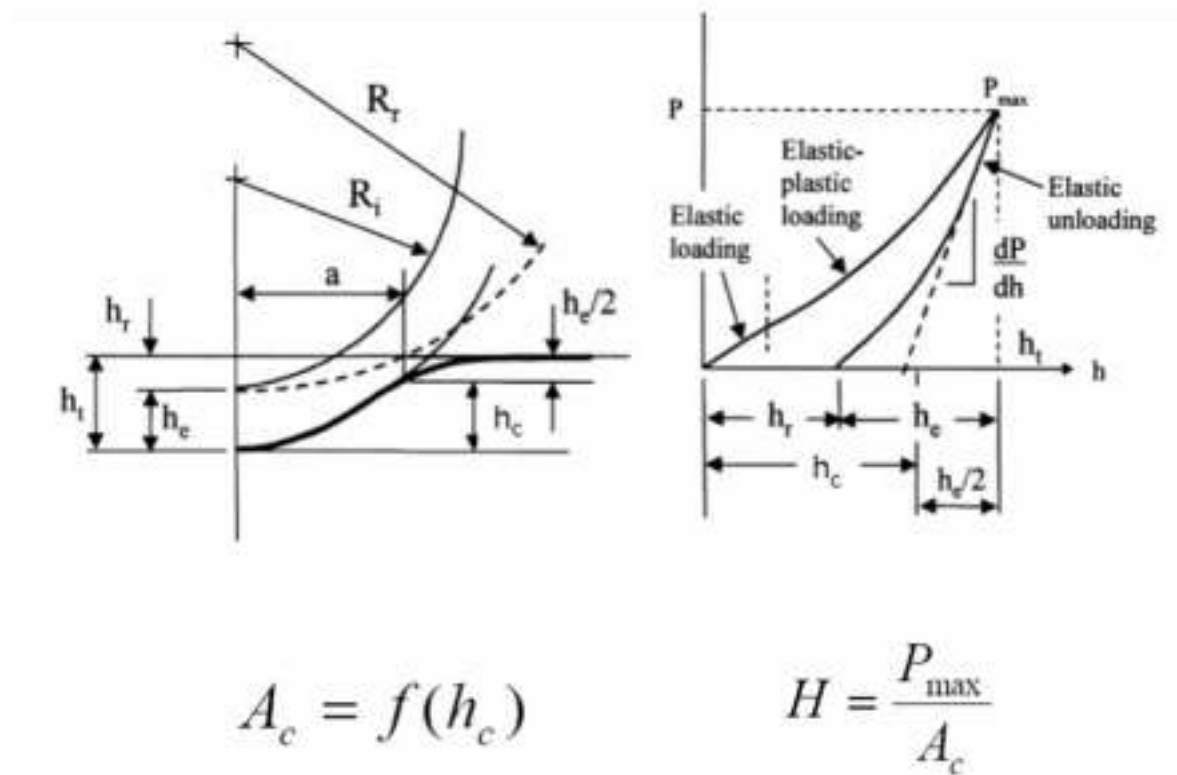
FIGURE 5.2 : DOERNER NIX MODEL

3. **Field Swan Model**: They extended the hertizian approach to incorporate plastic deformation in nanoindentation of an elastic half space of a sphere. They imagined that there exists an impression of depth h_f and its shape is that of the residual impression as would have been created by an actual indentation.

They proceed to consider that the whole process of nanoindentation is nothing but a reloading of the performed impression with the depth h_f into reconfirmation with the indenter.
Using a loading and partially unloading curve, the model could determine hardness and reduced modulus from the appropriate nanoindentation data.

Analytical Model – Field and Swain

$$P = \frac{4}{3} E_r R^{1/2} h^{3/2}$$

$$h_f = \frac{h_{part}\left(\frac{P_{max}}{P_{part}}\right)^{2/3} - h_{end}}{\left(\frac{P_{max}}{P_{part}}\right)^{2/3} - 1}$$

$$a = \sqrt{R(h_{end} + h_f) - \left(\frac{h_{end} + h_f}{2}\right)^2}$$
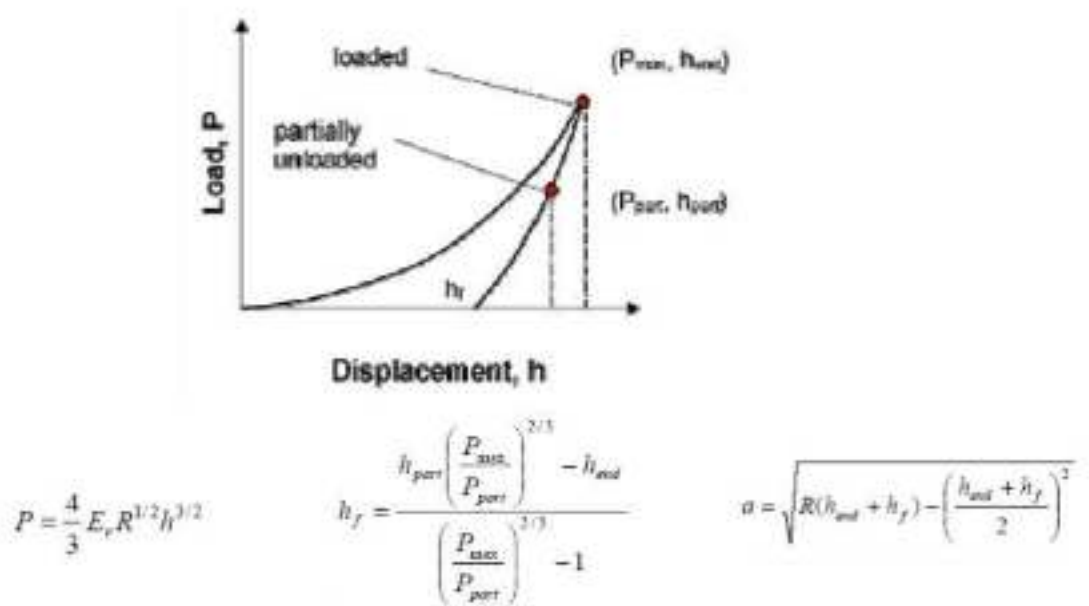
FIGURE 5.3: FIELD AND SWAN MODEL

CHAPTER 6

NANOINDENATION TECHQNIUES

Based on the load vs depth of penetration data generated, the parameters involved in nanoindentation experiment are given by h_f, the final depth of penetration ; h_{max} , the maximum depth of penetration of the indenter when $P=P_{max}$ and h_c , the contact depth , i.e. the displacement where the indenter has maximum contact with surface while unloading.

There are two area concepts used in nanoindentation in evaluation. If the area is calculated from contact depth, h_c , it is generally denoted by the contact area A_s.

There is another area called A_p , which is the projected area of an ideal nanoindenter. Since nanoindenters have very small tip radius, typically 40-200 Nm and the load may be ultralow, from a few micro newton to a few milli newton. The indentation imprints are also very small.

It is therefore difficult to measure contact area and contact height directly by experiment because of the elastic recovery. Therefore, these are calculated based on projected area A_p.

Assuming indenter has ideal shape and the surface it indents are perfectly flat , the contact depth is given by :-

$$h_c = \sqrt{\frac{A_p}{24.56}}$$

And when contact depth is known the contact area can be calculated as :-
$$A_c = 24.56 \, h_c^2$$

A_p can be measured from images of the indent. Once A_p is known, h_c can be calculated.

Because of repeated contact events and friction with the surface being indented, the tip of the nanoindenter gets worn out and is a result becomes rounded. Thereby shifting from its ideal shape. Hence calibration of the indenter area function is done to account for the deviation from ideal shape.

$$\text{Projected area: } A_p(h_c) = a_0 h_c^2 + a_1 h_c + a_2 h_c^{\frac{1}{2}} + a_3 h_c^{\frac{1}{4}} + \ldots + a_8 h_c^{\frac{1}{128}}$$

$$\text{Surface area: } A_s(h_c) = b_0 h_c^2 + b_1 h_c + b_2 h_c^{\frac{1}{2}} + b_3 h_c^{\frac{1}{4}} + \ldots + b_8 h_c^{\frac{1}{128}}$$

Thus from experimentally measured value of h_c using software packages, h_c is derived to reconstruct the fully loaded nanoindentation cavity surface from the residual nanoindentation cavity surface.

To improve accuracy of the nanoindentation results, the minimum and maximum height of the indent depth to be used for indenter area function calculation can be judiciously chosen in such a way as to avoid influences of the surface roughness & sharp tip area.
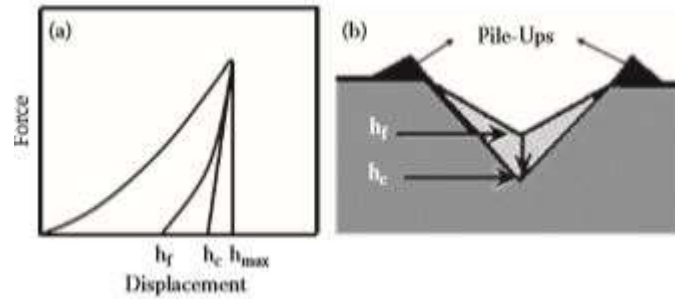
FIGURE 6.1: DEFINITION OF TYPICAL PHYSICAL PARAMETERS IN NANOINDENTATION: (a) LOAD (P) VERSUS DEPTH (H) PLOT; (b) CONCEPT OF CONTACT DEPTH (HC) AND FINAL DEPTH OF PENETRATION (HF).
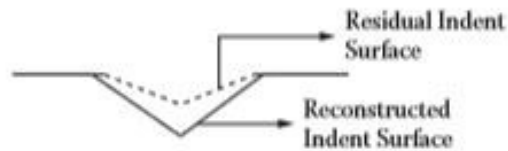
FIGURE 6.2: RECONSTRUCTED NANOINDENT CAVITY SURFACE AND THE RESIDUAL NANOINDENT CAVITY SURFACE.
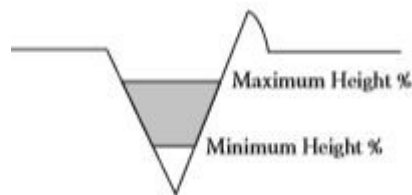
FIGURE 6.3: THE MINIMUM HEIGHT (%) AND THE MAXIMUM HEIGHT (%) THAT CAN BE USED TO IMPROVE THE ACCURACY OF RECONSTRUCTION

CHAPTER 7

INSTRUMENT DETAILS

The instrument is an IBIS Nanoindenter Model B having a dual load range of 0-50mN and 0-500mN. Dual Depth range of 0-2µm and 0-200µm.

Separate force and depth LVDT sensors are used. The force LVDT measures the deflection of accurately ground support springs to which is attached the indenter shaft. The depth LVDT measures the absolute displacement of the indenter shaft with respect to the load frame. In force feedback mode, the IBIS software establishes a set point for the desired force and the actuator expands until the force sensor output becomes equal to the set point. An overdamped active servo loop maintains the actuator expansion to keep the set point force a constant. A similar feedback mechanism is used in depth control for MEM's testing.
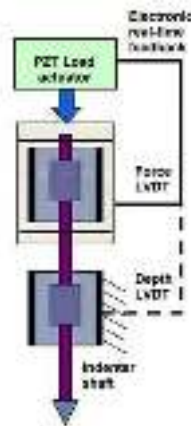
FIGURE 7.1: WORKING PRINCIPLE

FIGURE 7.2: IBIS NANOINDENTER

FIGURE 7.3: AN EXAMPLE OF A NANOINDENTER WITH ITS THREE PARTS: THE DIAMOND, THE HOLDER, AND THE BOND.
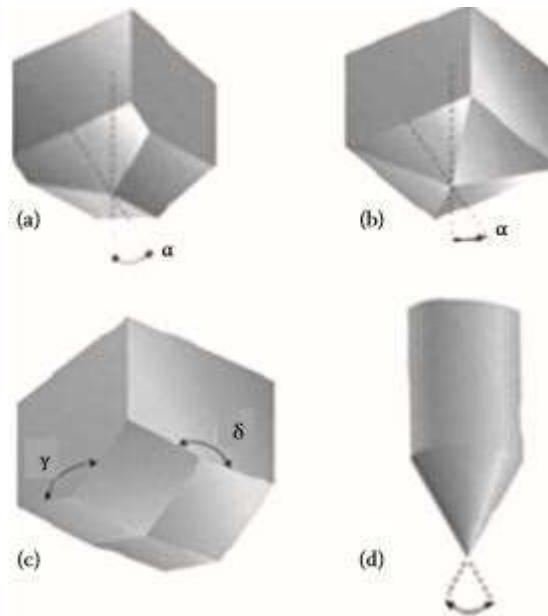
FIGURE 7.4: DIFFERENT TYPE OF INDENTERS: (A) BERKOVICH, (B) VICKERS, (C) KNOOP, AND (D) CONICAL.

CHAPTER 8

CALIBRATION & UNCERTAINTY

The instrument was calibrated using Fused Quartz for 4 different loads which are 1mN, 10mN, 25mN, 50mN.

Fused Quartz is used for calibration of the Nanoindenter because:-

Ultra-Pure(99.9%) having good thermal and mechanical properties.

Amorphous and isotropic in nature.

Cost- cheaper than sapphire and easy to make using quartz powder.

FIGURE 8.1: IBIS SOFTWARE

FIGURE 8.2: FUSED QUARTZ SAMPLE

It is known that the **Elastic Modulus of Fused Quartz is around 72.5 GPa** while the value of **hardness is expected to be 9 GPa**. Results have been analyzed for 1mN loading with 24 nanoindenation indents.

Analysis of p-h plot:

From the figure and table given below it can be clearly seen that loading and unloading curves overlap which means the instrument is well calibrated.
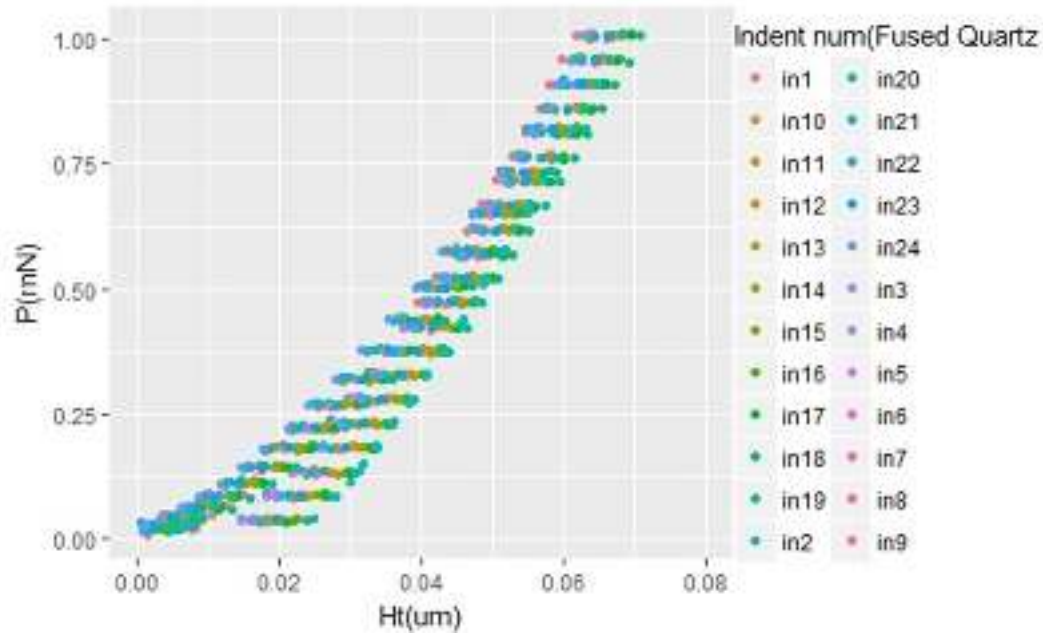
FIGURE 8.3: P-H PLOT

TERM	VALUE
Range(P in mN)	0.009872 - 1.01363
Range(Ht in um)	0.00034 - 0.0708
Standard deviation(P in mN)	0.3032315
Standard deviation(Ht in um)	0.0187622
Mean(P in mN)	0.4272911
Mean(Ht in um)	0.03680165

TABLE 8.1: P-H PLOT PARAMTER

Analysis of elastic modulus plot:

From the figure and the table below we see the range of Elastic modulus is from 66-75 GPa and mean is 70.7 GPa which means are instrument is well calibrated.

FIGURE 8.4: ELASTIC MODULUS PLOT

TERM	VALUE
Range(E in GPa)	66.00178 74.15085
Range(Ht in um)	0.00034 - 0.0708
Standard deviation(E in GPa)	2.125808
Standard deviation(Ht in um)	0.0187622
Mean(E in GPa)	70.07
Mean(Ht in um)	0.03680165

TABLE 8.2: ELASTIC MODULUS PARAMETERS

Analysis of hardness plot:

From the figure and table below it can be seen that the hardness range is around 8.5-9.1 GPa . The mean is 8.8 GPa which indicates that the instrument is well calibrated.
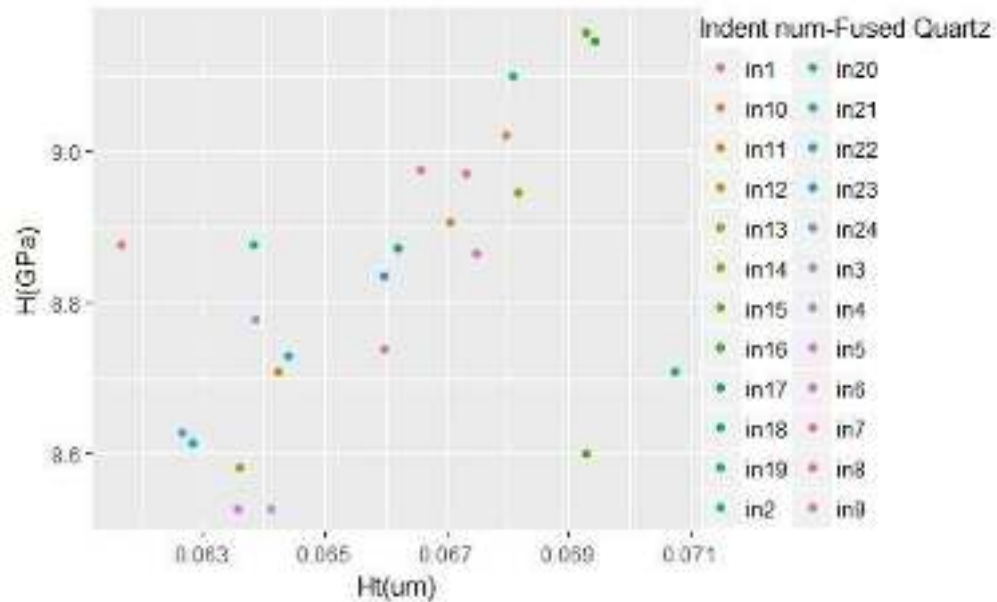
FIGURE 8.5: HARDNESS PLOT

TERM	VALUE
Range(H in GPa)	8.528315-9.158113
Range(Ht in um)	0.00034 - 0.0708
Standard deviation(H in GPa)	0.1883116
Standard deviation(Ht in um)	0.0187622
Mean(H in GPa)	8.820761
Mean(Ht in um)	0.03680165

TABLE 8.3: HARDNESS PARAMETERS

Creep:

The time dependent deformation plot is given below:-
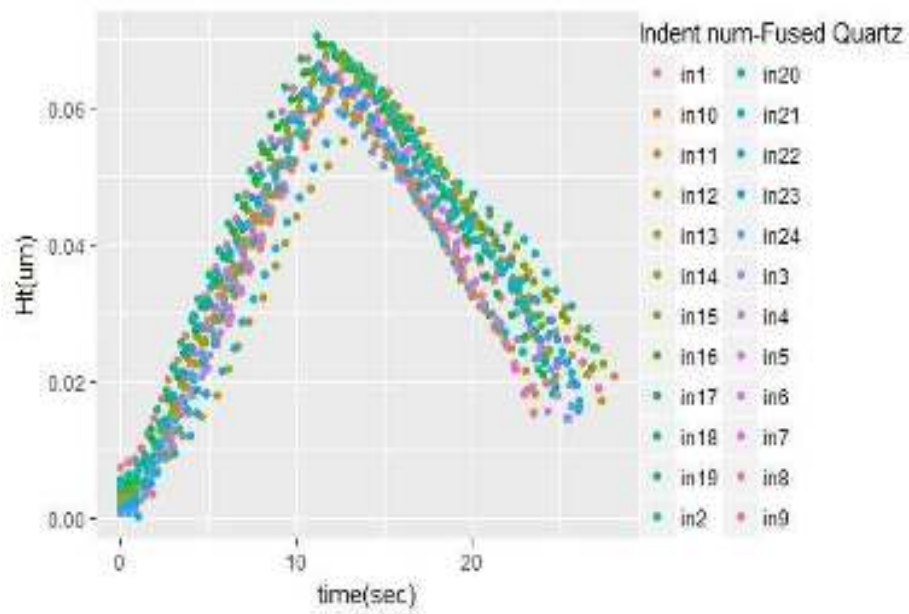
FIGURE 8.6: CREEP

TERM	VALUE
Range(Ht in um)	0.00034 - 0.0708
Range(time in sec)	0.000 - 28.125
Standard deviation(Ht in um)	0.0187622
Mean(Ht in um)	0.03680165

TABLE 8.4: CREEP PARAMETERS

Uncertainty Analysis:

Mean –(sum of observations/total number of observations)

Median- The median is the value separating the higher half of a data sample, a population, or a probability distribution, from the lower half.

Standard Deviation- it gives the dispersion or how scattered the data is

Residual- In simple terms it can be called the error in a result.(theortical-actual)

Regression analysis - regression analysis is a set of statistical processes for estimating the relationships among variables.

Curve fitting-curve fitting is the process of constructing a curve, or mathematical function that has the best fit to a series of data points, possibly subject to constraints.

Confidence interval (CI) is a type of interval estimate (of a population parameter) that is computed from the observed data.

Results obtained in R (statistical programming language)

The experimental results are corrected for the thermal drift of equipment system. The hardness and elastic modulus are determined by using the method of power law fitting between 100% and 20% of the unloading data.

$$P=\alpha(Ht-h_f)^m$$

where the constant α, hf, and m are determined by fitting the unloading data.

The table given on the next page shows the average of 24 nanoindentation indents. After analyzing the probability distribution of α, hf, and m we preliminarily hypothesize that hf may obeys the lognormal distribution and m may obey the normal distribution.

$$\ln\alpha \sim N(\mu_\alpha, \sigma_\alpha^2)$$

$$\ln h_f \sim N\left(\mu_{h_f}, \sigma_{h_f}^2\right)$$

$$m \sim N(\mu_m, \sigma_m^2)$$

Parameter	α	Hf(nm)	m	Pmax (mN)	Htmax(nm)
1	0.001902	17.2767	1.9719	1.001756	65.97533
2	0.001969	19.97974	1.85184	1.004255	66.5556
3	0.002068	21.09636	1.91743	1.006628	69.27312
4	0.001989	20.67533	2.00881	1.00794	67.96005
5	0.001811	19.53993	1.98385	1.009378	67.06734
6	0.001709	22.1436	1.87884	1.008191	64.23125
7	0.002073	20.79001	1.86665	1.007002	65.9823
8	0.002254	16.91528	1.9453	1.009129	68.1579
9	0.002206	22.38459	1.88708	1.002445	63.59497
10	0.001929	18.8938	1.9797	1.007943	69.42834
11	0.002371	19.55609	1.99453	1.009252	66.20492
12	0.002168	19.6348	1.9998	1.010315	69.28328
13	0.002483	19.47758	1.96211	1.009255	70.74511
14	0.001712	21.8435	1.92472	1.013626	68.08519
15	0.001627	20.9966	1.90872	1.006319	64.38132
16	0.001631	18.80561	1.98265	1.013626	68.08519
17	0.001948	18.85411	1.97851	1.009818	62.82234
18	0.001547	17.87353	1.95989	1.008629	61.63906
19	0.01463	16.48689	1.94919	1.01294	63.83136
20	0.001571	16.729	1.95219	1.010192	64.10522
21	0.001556	19.00615	1.98832	1.010378	63.55625
22	0.001817	20.41089	2.01668	1.006816	62.63886
23	0.001965	17.54671	1.96439	1.00663	67.49747
24	0.001452	17.45152	1.9706	1.009066	63.86226
Standard Deviation	0.0002875	1.705225	0.04571	0.002977	2.531816
Mean	0.0018842	19.34868	1.951821	1.008397	66.04017
Median	0.001939	19.50876	1.96325	1.96325	66.09361

TABLE 8.5: ESTIMATED PARAMETERS BY POWER LAW FITTING

A goodness of fit test by using the Kolmogorov-Smirnov and Monte Carlo simulation method are carried out. The comparison of empirical and theoretical fitted distributions for parameters distribution shows that the probability distributions of α, hf, and m fit the hypothesized distribution very well.
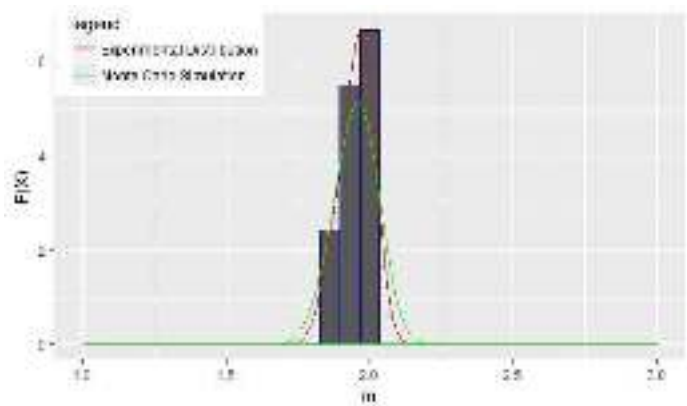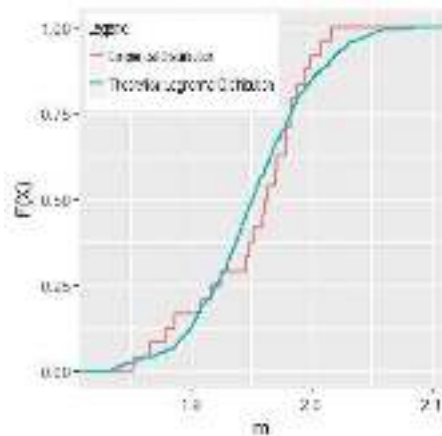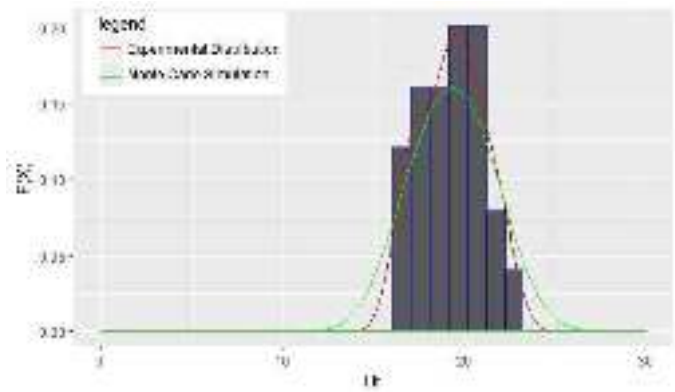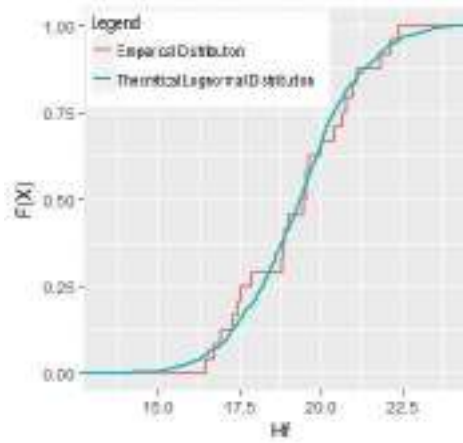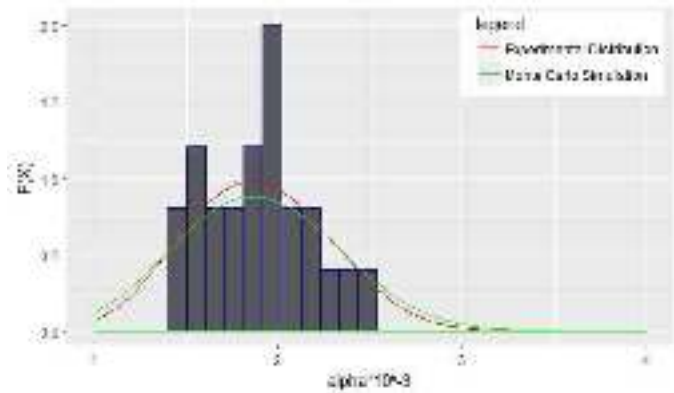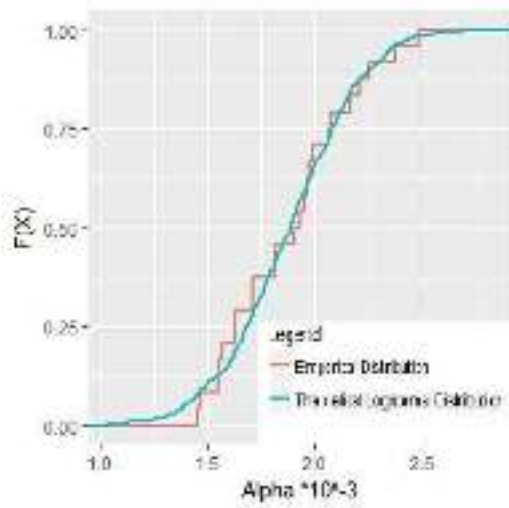
FIGURE 8.6: PARAMETER DISTRIBUTION. (LEFT SIDE) THE EMPIRICAL CDF DISTRIBUTION AND THEORETICAL CDF DISTRIBUTION OF THE HYPOTHESIZED FUNCTION; (RIGHT SIDE) COMPARISON OF EMPIRICAL AND THEORETICAL FITTED DISTRIBUTION.

The contact stiffness S is equals to the tangent at the maximum load i.e

$$S = \frac{dPmax}{dhmax} = m\alpha(h_{max}\text{-}h_f)^{m\text{-}1}$$

The value of ε depends on the indenter geometry. For a Berkovich indenter ε is 0.75

The contact depth can be given as :-

$$h_c = h_{max}\text{-}\varepsilon\left(\frac{Pmax}{S}\right)$$

Area calibration and uncertainty evaluation. The area calibration relates the actual, non-ideal diamond contact area to the depth of penetration. The target of the area calibration is to find the function which can be used across a wide indentation range to obtain accurate hardness and modulus values. In this study, the diamond area A is calculated using a polynomial function of order 2:

$$A = c_2 h_c^2 + c_1 h_c + c_0$$

For an ideal Berkovitch indenter, c2 = 24.5, c1 = c0 = 0. A real Berkovitch indenter, although each diamond is slightly different, the typical values are c2 = 20~24, c1 = 1500~3000. Here c2 = 22.81, c1 = 2430.6, and c0 = 51224.9.

Stiffness Uncertainty can be calculated as:-

$$
\begin{aligned}
[\mu(S)]^2 &= m\alpha(m-1)\left(h_{max} - h_f\right)^{m-2}\left[\mu(h_{max})^2 + \mu\left(h_f\right)^2\right] \\
&+ m\left(h_{max} - h_f\right)^{m-1}[\mu(\alpha)]^2 + \alpha ln(m-1)\left(h_{max} - h_f\right)[\mu(m)]^2
\end{aligned}
$$

The relative standard uncertainty for stiffness is given by:-

$$\left|\frac{\mu(s)}{s}\right| = 2.072\%$$

The uncertainty of contact depth is given as:-

$$[\mu(h_c)]^2 = [\mu(h_{max})^2] + [\frac{\varepsilon}{S}\mu(P_{max})]^2 + [\frac{\varepsilon}{S2}\mu(P_{max})\mu(S)]^2$$

The standard relative uncertainty of contact depth is given as :-

$$\left|\frac{\mu(hc)}{hc}\right| = 4.17\ \%$$

The uncertainty in area can be expressed as:-

$$[\mu(A)]^2 = (2h_c c_2 + c_1) \times [\mu(h_c)]^2 + \mu_\Delta^2$$

The standard relative uncertainty in area:-

$$\left|\frac{\mu(A)}{A}\right| = 7.41\%$$

The uncertainty of indentation hardness $\mu(H)$ can be obtained from equation :-

$$[\mu(H)]^2 = \left[\frac{1}{A}\mu(F_{max})\right]^2 + \left[\frac{F_{max}}{A^2}\mu(A)\right]^2$$

The relative standard uncertainty of indentation hardness is:-

$$\left[\frac{\mu(H)}{H}\right]^2 = \left[\frac{\mu(F_{max})}{F_{max}}\right]^2 + \left[\frac{\mu(A)}{A}\right]^2$$

$$= 10.18\%$$

PARAMETER	RELATIVE UNCERTAINTY
$\mu(S)$	2.072%
$\mu(hc)$	4.17%
$\mu(A)$	7.41%
$\mu(H)$	10.18%

TABLE 8.6: VALUES

CHAPTER 9

PECVD SYSTEM

MW PECVD technique: The indigenously built MW PECVD system used in the deposition and growth of carbon based nanostructures is shown in **Fig. 9.1** .The MW PECVD system consists of microwave power generator capable of generating maximum power of 1.2 kW and frequency 2.45 GHz. The chamber is composed of 300 series electro polished stainless steel. An isolator (PHILLIPS, model 02101) separates the magnetron from the other components and protects the magnetron from damage induced by the reflected microwaves. A detector is also associated with the isolator for measurement of reflected microwave power. Continuous water flow in the outer part of the circulator is used as load to take away the reflected microwave power by the heating process. Three stub tuners are used for impedance matching for delivering the maximum power. A wave guide (WR-340) is used to deliver the microwave power to the deposition chamber. The wave guide is rectangle to circulator mode convertor. The microwave components are separated from the deposition chamber by a quartz plate. The chamber is evacuated by the turbo molecular pump backed by the rotary pump combination. The microwave power is coupled to the process chamber by an iris coupling and the iris coupling is covered with a quartz plate. Heating is provided with the substrate by the resistive heating arrangement controlled by proportional integral derivative (PID). A silicon controlled rectifier has been used to deliver high power to the heating electrode. A negative substrate bias has been applied to substrate to attract the ion based species in the plasma. A generalize description of the different components of microwave system are given below.

FIGURE 10.1: PHOTOGRAPH OF MICROWAVE PECVD SYSTEM

Microwave generator: Microwave generators are designed to provide stable and controlled microwave power and are found in two configurations namely integrated and modular microwave system. We have modular system which consists of the separate building components, namely power supply, magnetron head, cable assembly, etc. It consists of a high voltage transformer, rectifier diode, capacitor, magnetron, waveguide for the process chamber.

High voltage transformer: The high voltage (HV) transformer has typically a secondary of around 2000 VRMS at 25 Ampere, more or less depending on the power rating of the magnetron. There is also a low voltage winding for the Magnetron filament (3.3 V at 10 A is typical). It is the largest and heaviest component of the generator. There is a pair of quick connect terminals for the AC input, a pair of leads for the magnetron filament and a single connection for the HV output. The HV return is fastened directly to the transformer frame and thus the chassis.

Rectifier: It is usually rated 12000 to 15000 peak reverse voltage at around 5 A. Most commonly, it is in rectangular or cylindrical shape and about 5 inches long with wire leads. In this generator a box bolted rectifier is used. One end of it is electrically connected to the chassis.

Capacitor: It is 0.65 to 1.2 µF at a working voltage of around 2000 V a. c. It is to be noted that this use of working voltage may be deceiving as the actual voltage on the capacitor may exceed this value during operation. The capacitor is a metal cased with quick connect terminals on top (one end).

Magnetron: Magnetron consists of a vacuum tube, electrons are emitted from a heating electrode (barium oxide coated tungsten) and attracted towards the anode which has relatively positive potential. A magnetic field aligned parallel to the electrode is applied to provide electrons spiral motion due to the magnetic force perpendicular to their motion. Synchronize radiation causes electrons to radiate microwaves. The frequency of microwave depends upon the size of the cavity. We are using magnetron (National Electronics Inc, USA, model YJ 1540) operating at 2.45 GHz of rating 1.2 KW.

Isolator/Circulator: A circulator is three port device utilizing ferrite technologies to selectively direct microwave energy to the specific port. An isolator is a circulator attached to a dummy load to one port. An isolator protects microwave generator from the reflected microwave energy and provides the magnetron a matched load for the generation of efficient microwave energy. Isolator (model PHILIPS, 2722 163 02101) with inbuilt detector (DD 1212) has been used in this system.

Three stub tuners: Stub tuners are mechanical waveguide component used for matching the impedance of the load and source to reduce reflected microwave energy and to deliver maximum power to the load. Tuners consist of metal stub which manipulates electromagnetic radiation inside

the waveguide. By adjusting the depth of metal stub into the waveguide, we change the capacitance, thus the properties of transmitting wave. By adjusting these metal stubs, microwave energy is tuned to give the minimum reflected power. The manually controlled three-stub tuner made by the National Electronics Inc, USA (model WR 340 tuner) is used in this system.

Waveguide: The size depends on the frequency and power of the microwave. The waveguide is typically made of aluminum, copper, stainless steel, etc. Aluminum is generally used to construct by aluminum due its low cost. In the present system, the waveguides (Al) having the dimensions (86.4 x 43.2 mm, wall thickness ~ 2 mm) is used (make: National Electronics Inc, USA, model WR 340 HBBSB).

CHAPTER 10

ANALYSIS OF CARBON NITRIDE COATING ON CARBON STEEL SAMPLE

Introduction: Carbon Steel Rings Used in the textile industries lack the robust qualities required and thus a suitable coating was required to enhance their mechanical properties. The Properties of carbon Steel (uncoated) and coated were studied using Nanoindentation. Furthermore for the coated samples uncertainty in Nanoindentation was evaluated and taken into account
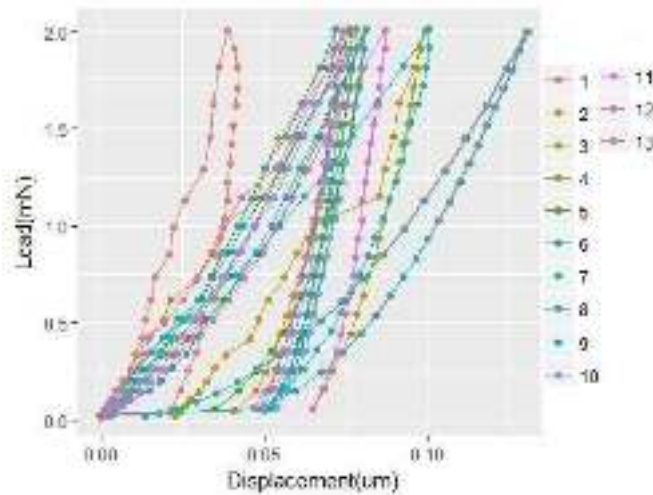
FIGURE 10. 1: LOAD DISPLACEMENT CURVE FOR CARBON STEEL SAMPLE
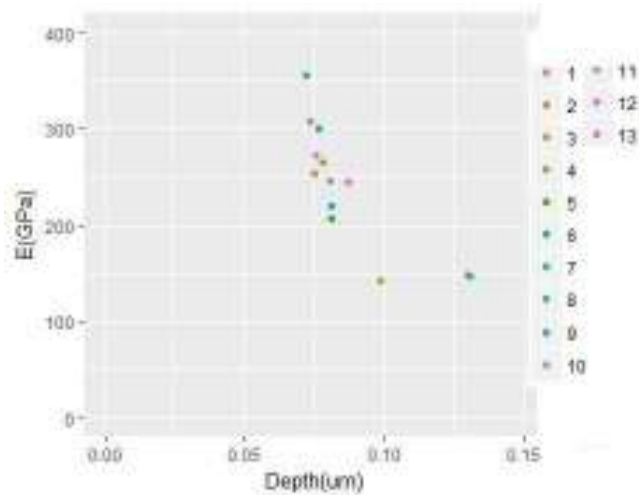
FIGURE 10.2: REDUCED MODULUS PLOT FOR CARBON STEEL SAMPLE
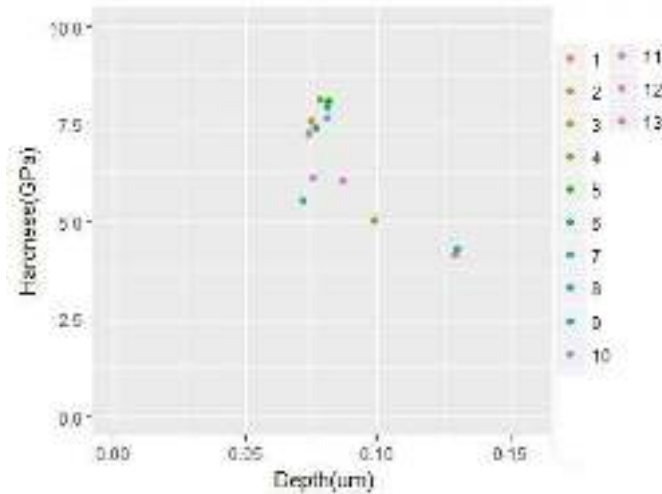
FIGURE 10.3: HARDNESS PLOT FOR CARBON STEEL SAMPLE

Parameter	Mean	Standard Deviation	Median
Load (mN)	0.841	0.6107	0.742
Hardness(GPa)	6.551	1.442	7.428
Reduced Modulus(GPa)	239.032	65.428	245.537

TABLE 10.1: PARAMETERS OF CARBON STEEL SAMPLE

Nanoindentation test for Carbon Steel Sample and Carbon Steel Sample with Carbon Steel Sample with Carbon Nitride Coating: The Nanoindentation test uses a diamond indenter (commonly known as berkovitch indenter) for probing mechanical properties like Hardness and Elastic Modulus. Further features include performing scratch test etc. The system used for Nanoindentation at CSIR-NPL is **IBIS NANOINDENTER type B.** In Nanoindentation, hardness may be defined as the mean pressure under the load.

$$H = \frac{P_{max}}{A}$$

Where P_{max} is the maximum load, A is the contact area and the contact depth can be calculated as

$$A = A(h_c) = 24.5h_c{}^2 + C_1h_c{}^1 + C_2h_c{}^{1/2} + C_3h_c{}^{1/4} + \cdots + C_8h_c{}^{1/128}$$

The Young's Modulus can be calculated as:

$$\frac{1}{E_r} = \frac{(1-v^2)}{E} + \frac{(1-v_i{}^2)}{E_i}$$

where E_r is the reduced modulus, E is the Young's modulus, v is the Poisson's ratio, and subscript i refers to the indenter.

A 13 indentation test was done on the sample whose results are summarized in **table 10.1.** From **table 10.1** we observe that the hardness is coming out to be 6.55 GPa while the reduced modulus is having a value of 239.02 GPa. The load displacement curve, reduced modulus plot and hardness are depicted in **figure 10.1, 10.2 and 10.3 respectively**

FIGURE 10.4: LOAD DISPLACEMENT CURVE FOR CARBON NITRIDE COATING ON CARBON STEEL

FIGURE 10.5: REDUCED MODULUS PLOT FOR CARBON NITRIDE COATING ON CARBON STEEL

FIGURE 10.6: HARDNESS PLOT FOR CARBON NITRIDE COATING ON CARBON STEEL

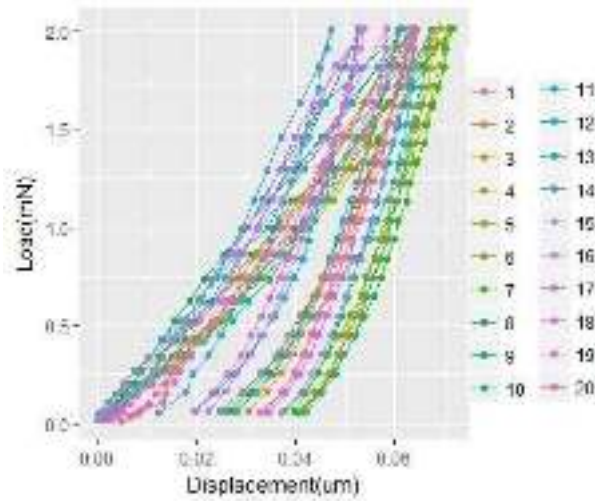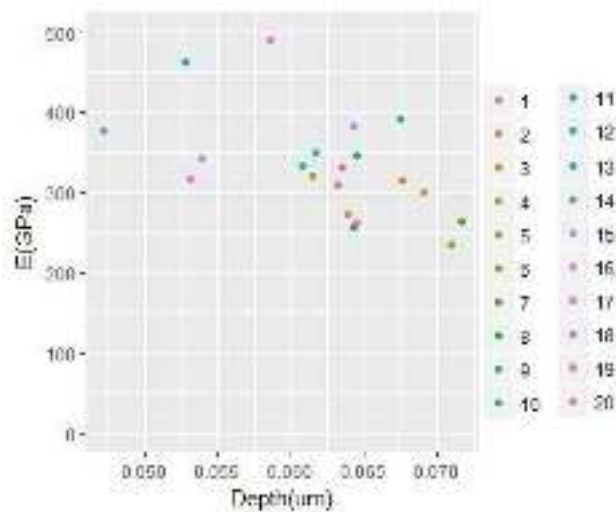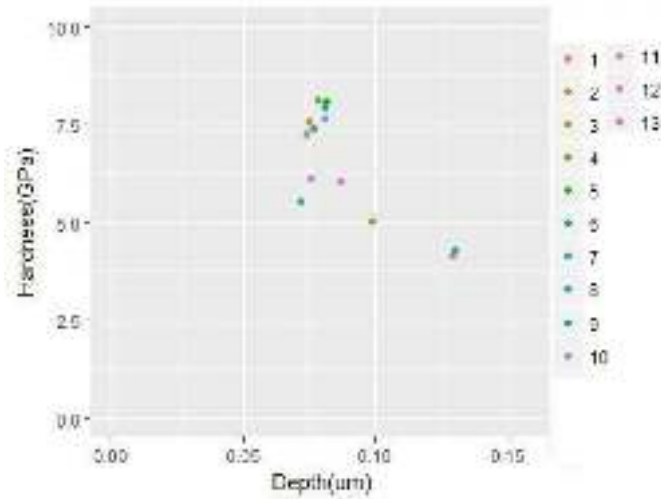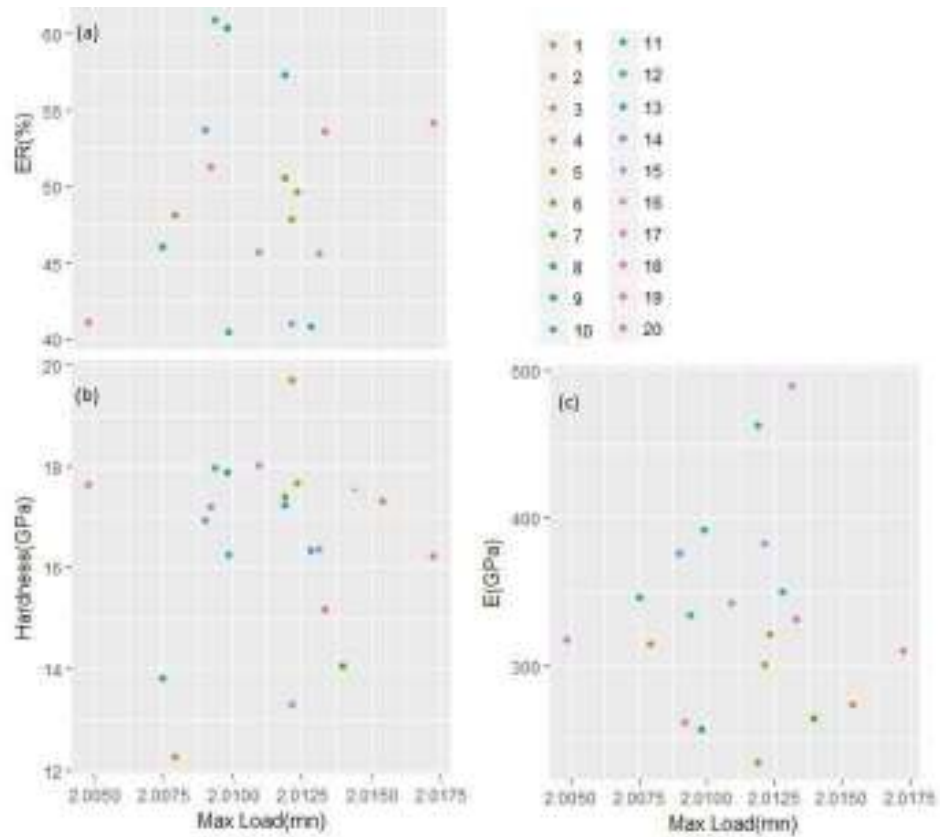**FIGURE 10.7: VARIATION OF (A) ELASTIC RECOVERY,(B) HARDNESS ,(C) REDUCED MODULUS OF CARBON NITRIDE COATED SAMPLE WITH RESPECT TO MAXIMUM LOAD**

Parameter	Mean	Standard Deviation	Median
Load(mN)	0.8408	0.611	0.742
Hardness(GPa)	16.436	1.851	17.061
Reduced Modulus(GPa)	333.189	65.37	326.197
Elastic Recovery(%)	50.875	7.73	50.094

TABLE 10.2: PARAMETERS OF CARBON NITRIDE COATED SAMPLE

The Carbon Steel sample was coated with Carbon Nitride using Plasma Enhanced Chemical Vapour Deposition technique (PECVD). A similar 20 indentation test was carried out on the coated sample and the results were summarized in **table 10.2.** From **table 10.2**, it can be seen that the reduced modulus increased from 239.02 GPa to 333.2 GPa. The load displacement curve, reduced modulus plot and hardness are depicted in **figure 10.4, 10.5 and 10.6 respectively**

Indent Number	α	h_f(nm)	m	h_{max}(nm)	P_{max}(mN)
1	0.006	28.70	1.631	63.19952	2.017257
2	0.0027	22.98	1.783	63.86495	2.015382
3	0.00319	35.07	1.847	67.61243	2.007946
4	0.0031	36.02	1.842	69.03818	2.012134
5	0.0048	30.96	1.911	61.48636	2.01232
6	0.0062	35.10	1.649	70.9688	2.011886
7	0.0055	24.93	1.752	71.62274	2.013947
8	0.0074	25.48	1.651	64.27207	2.009822
9	0.00532	34.78	1.831	64.4620	2.007509
10	0.0034	40.12	1.926	67.43321	2.009885
11	0.0027	23.76	1.828	60.74721	2.009384
12	0.0044	36.50	2.01	61.6581	2.01282
13	0.00353	22.53	1.855	52.82281	2.011883
14	0.00394	21.84	1.817	47.21751	2.00901
15.	0.0037	37.96	1.716	64.31124	2.012134
16.	0.00514	29.24	1.879	53.85687	2.010945
17.	0.0047	31.88	1.822	58.61167	2.013135
18.	0.00408	31.29	1.727	53.09641	2.004824
19	0.0029	29.41	1.881	63.43868	2.013321
20.	0.0062	31.42	1.836	64.51739	2.009196
Standard Deviation	0.001349	5.527	0.098025	6.383951	0.002876
Mean	0.00445	30.512	1.8097	62.21191	2.011237
Median	0.00424	31.125	1.8295	63.65182	2.011885

TABLE 10.3: ESTIMATED PARAMETERS BY POWER LAW FITTING FOR CARBON NITRIDE COATED SAMPLE

Parameter	A	h_f	M
Mean	0.00445	30.512	1.8097
Interval	[0.0039,0.00497]	[28.30,32.72]	[1.771,1.849]

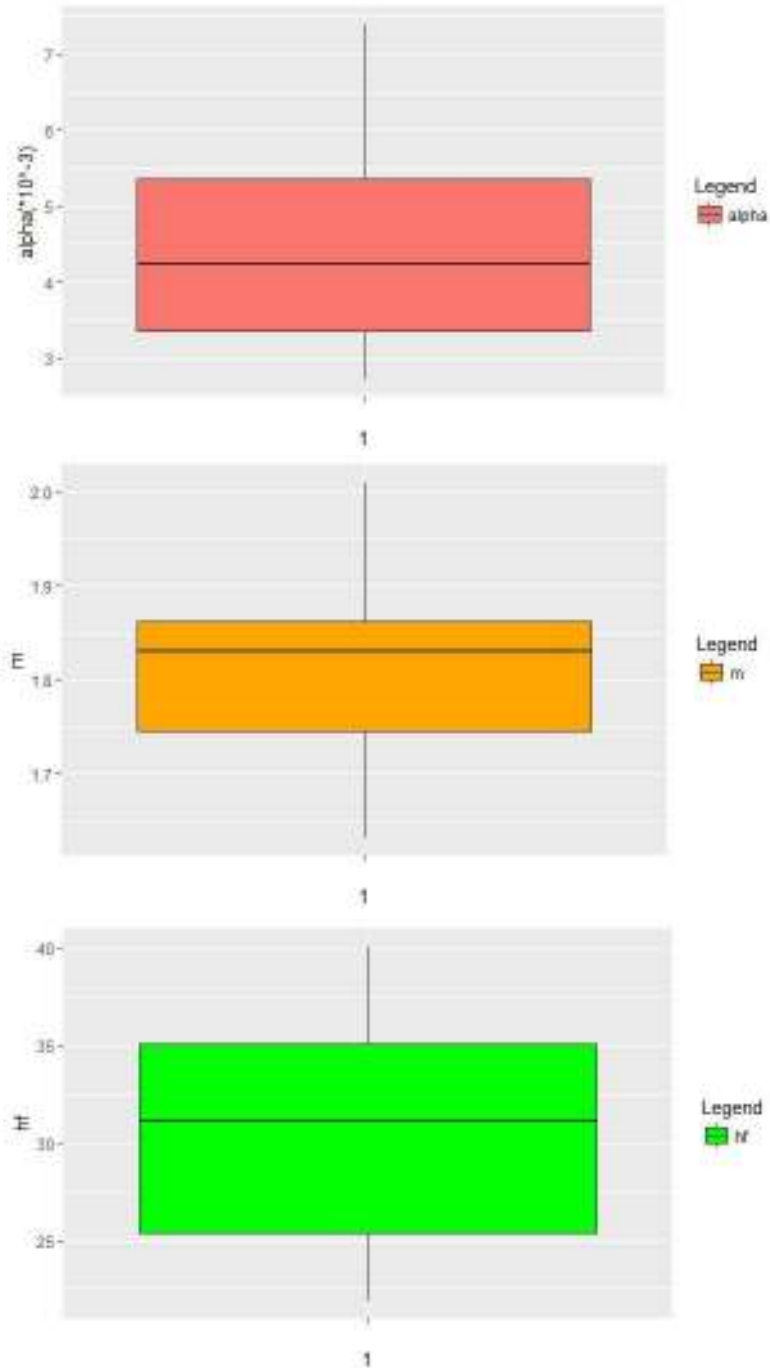**TABLE 10.4: 95% CONFIDENCE INTERVAL BY PARAMETRIC BOOTSTRAP METHOD**
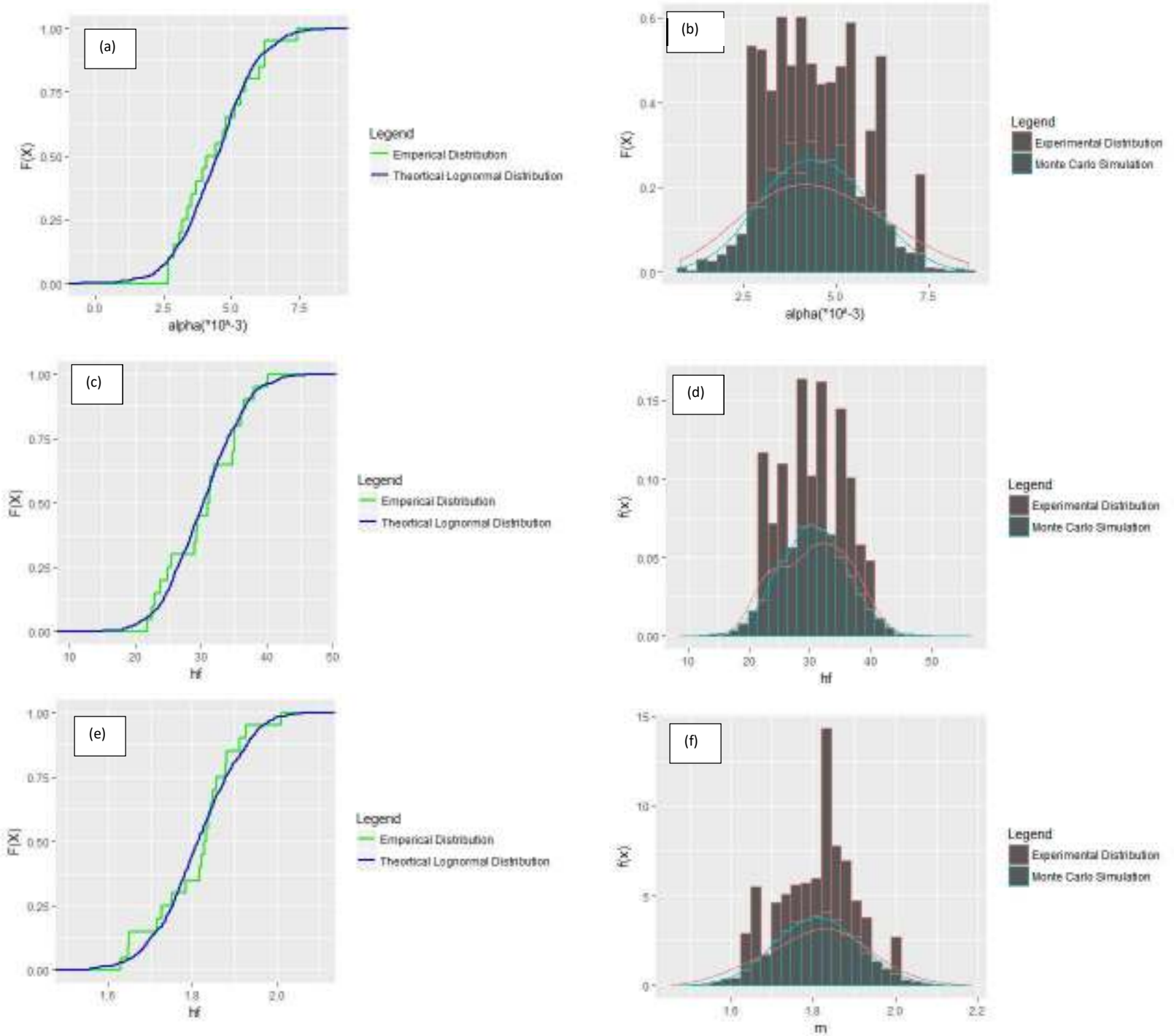

FIGURE 10.8: BOXPLOT OF α, m AND h_f

FIGURE 10.9: (A, C, E) THE EMPIRICAL CDF DISTRIBUTION AND THEORETICAL CDF DISTRIBUTION OF THE HYPOTHESIZED FUNCTION; (B, D, F) COMPARISON OF EMPIRICAL AND THEORETICAL FITTED DISTRIBUTION

Experimental Results:

Doerner observed that for some materials, the initial portions of unloading curves are linear, and the unloading stiffness is then related the modulus and contact area through the relationship:

$$S = \frac{dP}{dh} = \frac{2}{\sqrt{\pi}} E_r \sqrt{A}$$

where, S = dP/dh is the initial unloading stiffness obtained by the initial portion of the unloading process. A is the projected area of the elastic contact. It is assumed that the contact area between the indenter and the material remains constant and moves elastically during unloading, and the plastic area is always equal to the contact area.

The experimental results are corrected for thermal drift. The hardness and elastic modulus is calculated using the power law fitting method of the unloading curve.

$$P = \alpha(h - h_f)^m$$

α, h_f and m are fitting constants whose value can be determined from the upper half of the unloading curve.

Parameter Distribution Analysis: Figure 10.8 gives the range and distribution of α,h_f and m in the form of boxplots.**Table 10.3** represents the average test results of 20 indent runs performed on the Carbon Steel sample coated with Carbon Nitride. It can be hypothesized about α,h_f and m that α and h_f obey the lognormal distribution but m obeys the normal distribution.

$$ln\ \alpha \sim N(\mu_\alpha, \sigma^2_\alpha)$$

$$ln\ h_f \sim N\left(\mu_{h_f}, \sigma^2_{h_f}\right)$$

$$m \sim N(\mu_m, \sigma^2_m)$$

Since the number of indents (n=20) are small, so to test whether parameters α, h_f and m in **Table 10.3** follow the expected probability distribution, a goodness of fit test by using the Kolmogorov-Smirnov and Monte Carlo simulation method are conducted. The comparison between the theoretical and empirical distribution is done in **FIG 9** and shows that the probability distribution of α,h_f and m fit the hypothesized distributions very well.

Uncertainty estimation for reduced modulus and hardness of Carbon Nitride Coated Sample: The mechanical properties of the Carbon Nitride Coated sample are Hardness and Reduced Modulus. The contact area is calculated from the contact depth h_c which is related to the total displacement h_{max} of the indenter as:

$$h_c = h_{max} - \varepsilon\left(\frac{P_{max}}{S}\right)$$

Here S is the Contact Stiffness and ε is a constant whose value depends upon the indenter geometry. For a standard Berkovich Indenter, the value of ε is 0.75.

The Contact Stiffness can be defined as the tangent at the maximum load :

$$S = \frac{dP_{max}}{dh_{max}} = m\alpha(h_{max} - h_f)^{m-1}$$

Area calibration and uncertainty evaluation: The area calibration is the relation between the actual, non-ideal diamond contact area to the depth of penetration. The diamond area (A) can be approximately calculated using a polynomial function of order 2:

$$A = c_2 h_c^{\,2} + c_1 h_c + c_0$$

For an ideal Berkovitch Indenter c_2=24.5, c_1=c_0=0. However, for a real Berkovitch Indenter, the typical values are c_2=20-24, c_1=1500-3000(although each diamond is unique). Here $c_2 = 22.81$, $c_1 = 2430.6$, and $c_0 = 51224.9$.

The standard area uncertainty μ(A) can be calculated using the uncertainty propagation law :

$$[\mu(A)]^2 = (2c_2 h_c + c_1) \times [\mu(h_c)]^2 + \mu_\Delta^{\,2}$$

Where $\mu_\Delta^{\,2}$ is the residuals from the fitting curve, $\mu(h_c)$ is the uncertainty of depth which can be calculated by:

$$[\mu(h_c)^2] = [\mu(h_{max})^2] + \left[\frac{\varepsilon}{S}\mu(P_{max})^2\right] + \left[\frac{\varepsilon}{S^2}\mu(P_{max})\mu(s)\right]^2$$

Where $\mu(h_{max})$ is the maximum depth uncertainty, $\mu(P_{max})$ is the uncertainty of maximum applied load, ε is a constant with value 0.75 and $\mu(s)$ is uncertainty in contact stiffness which can be calculated as below:

$$\mu(S)^2 = m\alpha(m-1)(h_{max} - h_f)^{m-2}\left|\mu(h_{max})^2 + \mu(h_f)^2\right| + m(h_{max} - h_f)^{m-1}[\mu(\alpha)^2]$$
$$+ \alpha ln(m-1)(h_{max} - h_f) + [\mu(m)^2]$$

In this experiment, the maximum load uncertainty $\mu(P_{max})$ and the maximum depth uncertainty $\mu(h_{max})$ are calculated by the standard deviation of the 20 nodes test done on the sample of carbon steel coated with carbon nitride. As it is earlier stated that α and h_f follow a lognormal distribution while m follows a normal distribution, the uncertainty can be calculated as the root of variance. $\mu(\alpha)$ =0.001349, $\mu(h_f)$ = 5.527 nm and $\mu(m)$ = 0.098025. The uncertainty of maximum load and maximum depth are $\mu(P_{max})$ =0.002876 and $\mu(h_{max})$ =6.384 nm. Therefore:

$$\mu(S) = 5.406 \, nm$$

The relative standard contact stiffness uncertainty $\left[\frac{\mu(S)}{S}\right]$ can be found as:

$$\left[\frac{\mu(S)}{S}\right] = \frac{5.406}{132.2} = 4.09\%$$

Therefore:

$$\mu(h_c) = 6.32 \, nm$$

The relative standard contact depth uncertainty $\left[\frac{\mu(h_c)}{h_c}\right]$ can be found as:

$$\left[\frac{\mu(h_c)}{h_c}\right] = \frac{6.32}{62.198} = 10.27\%$$

$$\mu(A) = 3213.43 \, mn^2$$

The relative standard area uncertainty $\left[\frac{\mu(A)}{A}\right]$ can be found as:

$$\left[\frac{\mu(A)}{A}\right] = \frac{3213.43}{141932.1} = 2.27\%$$

Uncertainty of Hardness: The uncertainty of hardness for indentations can be calculated as follows:

$$[\mu(H)]^2 = \left[\frac{\mu(P_{max})}{A}\right]^2 + \left[\frac{P_{max}}{A^2}\mu(A)\right]^2$$

The relative standard hardness uncertainty can be calculated as:

$$\left[\frac{\mu(H)}{H}\right]^2 = \left[\frac{\mu(P_{max})}{P_{max}}\right]^2 + \left[\frac{\mu(A)}{A}\right]^2$$

The relative expanded uncertainty of hardness for a level of 95% is given as:

$$U(H) = 2 \times \frac{u(H)}{H} = 6.81\%$$

Uncertainty of Reduced Modulus: The uncertainty of reduced modulus for indentations can be calculate as follows:

$$[\mu(E)]^2 = \left[\frac{\sqrt{\pi}}{2}\frac{1}{\sqrt{A}}\mu(s)\right]^2 + \left[\frac{\sqrt{\pi}}{4}\frac{S}{A^{3/2}}\mu(A)\right]^2$$

The relative standard uncertainty of reduced modulus can be calculated as:

$$\left[\frac{\mu(E)}{E}\right]^2 = \left[\frac{\mu(S)}{S}\right]^2 + \left[\frac{1}{2}\frac{\mu(A)}{A}\right]^2$$

The relative expanded uncertainty of reduced modulus for a level of 95% is given as:

$$U(E) = 2 \times \frac{\mu(E)}{E} = 8.5\%$$

CHAPTER 11

USING R AS AN EFFECTIVE TOOL FOR CALCULATING UNCERTAINTY IN NANOINDENTATION

R is a programming language and free software environment for all statistical computing and graphics that is supported by the R Foundation for Statistical Computing. The R language is widely used among statisticians and data miners for developing statistical software and data analysis. Polls, surveys of data miners, and studies of scholarly literature databases show that R's popularity has increased substantially in recent years. As of May 2018, R ranks 11th in the TIOBE index, a measure of popularity of programming languages.

R is a package. The source code for the R software environment is written primarily in C, Fortran, and R. R is freely available under the GNU General Public License, and pre-compiled binary versions are provided for various operating systems. While R has a command line interface, there are several graphical front-ends and integrated development environments available. R is an implementation of the S programming language combined with lexical scoping semantics inspired by Scheme. S was created by John Chambers in 1976, while at Bell Labs. There are some important differences, but much of the code written for S runs unaltered.

R was created by Ross Ihaka and Robert Gentleman at the University of Auckland, New Zealand, and is currently developed by the *R Development Core Team*, of which Chambers is a member. R is named partly after the first names of the first two R authors and partly as a play on the name of S. The project was conceived in 1992, with an initial version released in 1995 and a stable beta version in 2000.**It is preferred that RStudio should be used for R**.

FIGURE 11.1: RStudio and R LOGO

Statistical Features of R: and its libraries implement a wide variety of statistical and graphical techniques, including linear and nonlinear modeling, classical statistical tests, time-series analysis, classification, clustering, and others. R is easily extensible through functions and extensions, and the R community is noted for its active contributions in terms of packages. Many of R's standard functions are written in R itself, which makes it easy for users to follow the algorithmic choices made. For computationally intensive tasks, C, C++, and Fortran code can be linked and called at run time. Advanced users can write C, C++, Java, .NET or Python code to manipulate R objects directly. R is highly extensible through the use of user-submitted packages for specific functions or specific areas of study. Due to its S heritage, R has stronger object-oriented programming facilities than most statistical computing languages. Extending R is also eased by its lexical scoping rules.

Another strength of R is static graphics, which can produce publication-quality graphs, including mathematical symbols. Dynamic and interactive graphics are available through additional packages.

R has Rd, its own LaTeX-like documentation format, which is used to supply comprehensive documentation, both on-line in a number of formats and in hard copy.

Using R for Uncertainty in Nanoindentation: The Excel Files received from the Nano indentation instrument can be imported in R and then their analysis can be carried out.

#For performing curve fiiting in R the nls function can be used and a sample code has been given:

> rhs <- function(x, b0, b1) { + b0 + x^b1 + } >

 m.2 <- nls(y ~ rhs(x, intercept, power), data = ds, start = list(intercept = 0, + power = 2), trace = T) 9

> summary(m.2) Formula: y ~ rhs(x, intercept, power)

> plot(ds$y ~ ds$x, main = "Fitted power model, with intercept", + sub = "Blue: fit; magenta: fit w/o intercept; green: known")

 > abline(h = 0, lty = 1, lwd = 0.5) > lines(s, s^3, lty = 2, col = "green") > lines(s, predict(m.2, list(x = s)), lty = 1, col = "blue") > lines(s, predict(m, list(x = s)), lty = 2, col = "magenta") > segments(x, y, x, fitted(m.2), lty = 2, col = "red")
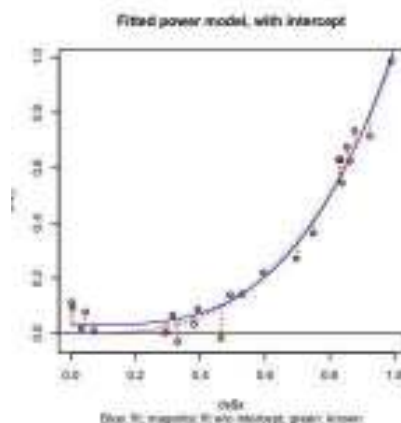
#The code to perform the Kolmogorov–Smirnov test (KS Test) using the ggplot 2 function is given below:

```
> ggplot(dat, aes(x = KSD, group = group, color = group))+stat_ecdf( size=1)+xlab("Sample") +
ylab("ECDF")
> sample1 <- m$hf
>  sample2 <- rnorm(1000, 30.512, 5.572)
>  group <- c(rep("sample1", length(sample1)), rep("sample2", length(sample2)))
>  dat <- data.frame(KSD = c(sample1,sample2), group = group)
>  # create ECDF of data
>   cdf1 <- ecdf(sample1)
>   cdf2 <- ecdf(sample2)
>   ggplot(dat, aes(x = KSD, group = group, color = group))+stat_ecdf( size=1)+xlab("Sample")
+ylab("ECDF")
```

 # The code to perform Monte Carlo Simulation is given below:

```
> sample1 <- m$hf
>  sample2 <- rnorm(1000, 30.512, 5.572)
>  group <- c(rep("sample1", length(sample1)), rep("sample2", length(sample2)))
>  dat <- data.frame(KSD = c(sample1,sample2), group = group)
>  # create ECDF of data
>   cdf1 <- ecdf(sample1)
>   cdf2 <- ecdf(sample2)
>   ggplot(dat, aes(x= KSD, group = group, color = group))+geom_histogram(aes(y=..density..))
+geom_density(adjust=2)+xlab("Sample") +ylab("")
```
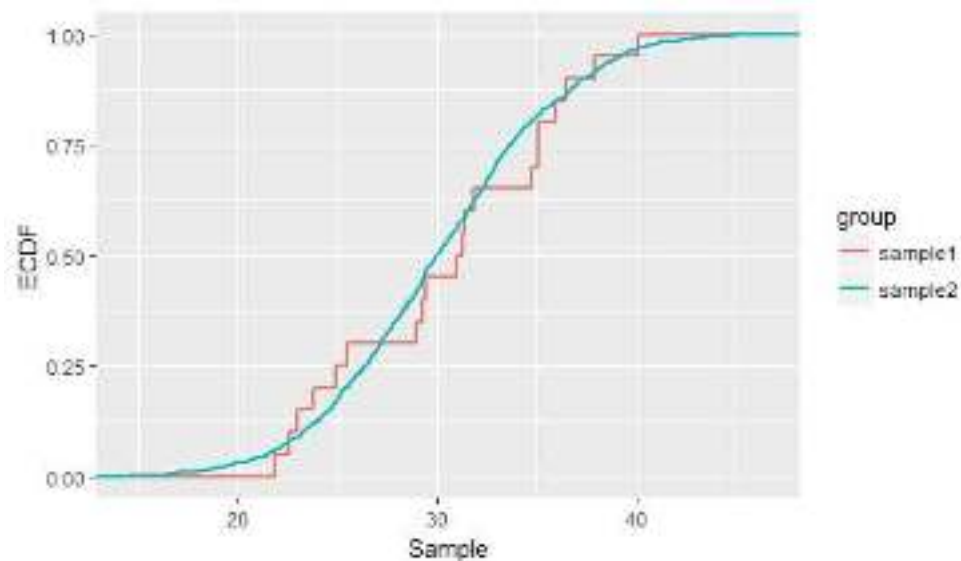

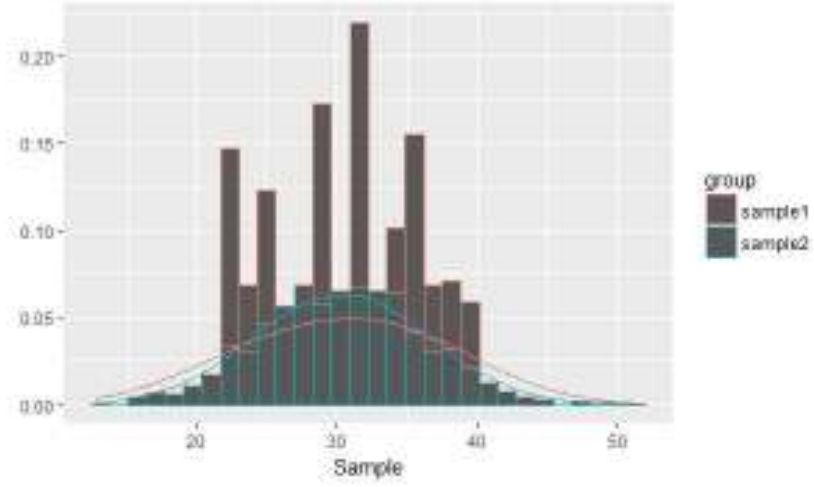**FIGURE 11.2 : KS TEST SAMPLE RUN**

FIGURE 11.3:MONTE CARLO SIMULATION

Rest equations given below for uncertainty can be solved in R following general programming conventions of the language

$$[\mu(A)]^2 = (2c_2 h_c + c_1) \times [\mu(h_c)]^2 + {\mu_\Delta}^2$$

$$[\mu(h_c)^2] = [\mu(h_{max)}^2] + \left[\frac{\varepsilon}{S}\mu(P_{max})^2\right] + \left[\frac{\varepsilon}{S^2}\mu(P_{max})\mu(s)\right]^2$$

$$\mu(S)^2 = m\alpha(m-1)(h_{max} - h_f)^{m-2}|\mu(h_{max})^2 + \mu(h_f)^2| + m(h_{max} - h_f)^{m-1}[\mu(\alpha)^2]$$
$$+ \alpha ln(m-1)(h_{max} - h_f) + [\mu(m)^2]$$

$$\left[\frac{\mu(H)}{H}\right]^2 = \left[\frac{\mu(P_{max})}{P_{max}}\right]^2 + \left[\frac{\mu(A)}{A}\right]^2$$

$$\left[\frac{\mu(E)}{E}\right]^2 = \left[\frac{\mu(S)}{S}\right]^2 + \left[\frac{1}{2}\frac{\mu(A)}{A}\right]^2$$

CONCLUSION AND FUTURE SCOPE

The uncertainty of hardness and reduced modulus have been evaluated up to a 95% confidence level.The results of the uncertainty analysis have been summarized in the **table C.1**. The experimental results and uncertainty analysis reveal that the relative expanded uncertainty of hardness and reduced modulus of carbon nitride coated sample corresponding to a level of confidence of 95% are separately 6.81% and 8.5%. The uncertainty analysis also shows that nanoindentation is an effective technique in determining the mechanical properties of carbon nitride coated samples. Not only does the carbon nitride coating improve mechanical properties like hardness and reduced modulus but also adds aesthetic features as well to the carbon steel sample which can be observed from the **picture C.1.**

Furthermore this coating may be used on other metallic samples and then its analysis should be carried out.

Parameter	Relative Expanded Uncertainty
$\mu(A)$	4.54%
$\mu(H)$	6.81%
$\mu(E)$	8.5%

TABLE C.1: THE RELATIVE EXPANDED STANDARD UNCERTAINTY OF PARAMETERS WITH A LEVEL OF CONFIDENCE OF 95%.

FIGURE C.1: COMPARISION BETWEEN COATED AND UNCOATED SAMPLE

REFERENCES

1. Anthony Fischer-Cripps(2002), -Nanoindentation, springer mechanical engineering series

2. Jaroslav Menčík (2012),Uncertainties and Errors in Nanoindentation ,Intech Open

3. CP Robert(2009), Introducing Monte Carlo Methods with R , Springer

4. Xingling Tang(2017) ,Elastic properties of single-walled carbon nanotube thin flm by nanoindentation test, Nature Scientific Reports

5. Arjun Dey,Nanoindentation of Brittle Solids, CRC Press

6. R Core Team (2017). R: A language and environment for statistical computing. R Foundation for Statistical Computing, Vienna, Austria. URL-https://www.R-project.org/.

7. H. Wickham. ggplot2: Elegant Graphics for Data Analysis. Springer-Verlag New York, 2009.